SPIRE-ALC-DOC-002357

ALCATEL SPACE

HERSCHEL / PLANCK

Herschel/Planck EMC analyses

Product Code : 000000

Written by	*Responsibility-Office -Company*	Date	Signature
L. TROUGNOU	EMC engineer	03/05/02	
Verified by			
K. HIBBERD	Electrical Interfaces manager	3/5/02	
P. COUZIN	Electrical Architecture manager	3/5/02	
Approved by			
P. RIDEAU	Engineering manager	17/05/02	
C. MASSE	PA manager	23/05/02	
J.J. JUILLET	Project manager	22/05/02	

DATA MANAGEMENT:

Entité Emettrice : Alcatel Space - Cannes
(détentrice de l'original) :

HERSCHEL/PLANCK	**DISTRIBUTION RECORD**		
DOCUMENT NUMBER : H-P-1-ASPI-AN-202		Issue 1 / Rev. : Date: 03/05/2002	
EXTERNAL DISTRIBUTION		**INTERNAL DISTRIBUTION**	
ESA	**X**	**HP team**	**X**
ASTRIUM	**X**		
ALENIA	**X**		
CONTRAVES			
TICRA			
TECNOLOGICA			
		Clt Documentation	**Orig.**

ENREGISTREMENT DES EVOLUTIONS / CHANGE RECORDS

ISSUE	DATE	§ : DESCRIPTION DES EVOLUTIONS § : CHANGE RECORD	REDACTEUR AUTHOR
1	03/05/2002	Initial issue	

TABLE OF CONTENTS

1. SCOPE

The purpose of this document is to present a synthesis of the various EMC analyses carried out before Herschel/Planck System PDR.

In the first chapters of this document, classical system EMC analyses are presented :

- CS/CE compatibility on primary power lines
- RF compatibility analyses (spacecraft self-compatibility and compatibility with launcher)

The second part of the document is a summary of ASPI knowledge and understanding of the Instruments (considered as the System EMC drivers) EMC-related design and characteristics :

- Instruments noise specifications
- Instruments detection chains grounding and EMC concepts

The general principles of detection chains protection against low frequency and high frequency EMI will be presented and the Instruments detection chains grounding/shielding strategies will be commented and assessed with reference to those general principles.

No specific EMC simulation (e.g. using network simulation software) of the detection chains will be presented as this is on going under the Instruments responsibility, with PSPICE for most of them. However, general advice on the way to treat the detection chains EMI rejection assessments (included with PSPICE) will be given whenever relevant.

In the end, ASPI design baseline for cryo-harness protection against ESD will be presented and assessed.

2. DOCUMENTS

2.1 Applicable documents

[AD-01] First/Planck System Requirements Specification (SRS), SCI-PT-RS-05991

[AD-02] IID Part A, SCI-PT-IIDA-04624

[AD-03] IID Part B, Bolometer Instrument, SCI-PT-IIDB/SPIRE-02124

[AD-04] IID Part B, Heterodyne Instrument, SCI-PT-IIDB/HIFI-02125

[AD-05] IID Part B, Photoconductor Instrument, SCI-PT-IIDB/PACS-02126

[AD-06] IID Part B, HFI, SCI-PT-IIDB/HFI-04141

[AD-07] IID Part B, LFI, SCI-PT-IIDB/HFI-04142

[AD-08] Ariane 5 user manual, Issue 3/Rev. 00 - March 2000

[AD-09] General Design and Interface Requirements, H-P-1-ASPI-SP-0027

[AD-10] EMC Specification, H-P-1-ASPI-SP-0037

[AD-11] EMC/ESD Control Plan, H-P-1-ASPI-PL-0038

2.2 Reference documents

2.2.1 Reference articles and books

- Semiconductor failure threshold estimation problem in electromagnetic assessment, IEEE Transactions on Nuclear Science, Vol. NS-31, N° 6, December 1984, E. W. Enlow and D. C. Wunsch
- EMI Control Methodology and Procedures, Don White
- Manuel pratique de compatibilité électromagnétique, Michel Mardiguian
- Electrostatic Discharge, Understand, Simulate and Fix ESD problems, Michel Mardiguian

2.2.2 EMC analyses

[AN-1] Cryostat Shielding Efficiency Assessment Consolidation, H-P-2-ASPI-TN-0177, 30/11/2001
[AN-2] Filtering of FCU – IF amplifiers interface SRON-U/FCU/TN/2000-003, Draft2
[AN-3] HIFI EMI sensitivity estimate (worksheet), 02/07/2001
[AN-4] Report on HIFI EMC Status, SRON-G/HIFI/RP/2001-001

2.2.3 EMC/Power Working Group minutes

[WG-11] EMC/Power WG meeting #11, H-P-ASPI-MN-306, 29/08/2001
[WG-H1] EMC WH Herschel/Cryostat, H-P-ASPI-MN-311, 30/08/2001
[WG-12] EMC/Power WG meeting #12, H-P-ASPI-MN-534, 06/11/2001
[WG-13] EMC/Power WG meeting #13, H-P-ASPI-MN-810, 16/01/2002
[WG-P1] Dedicated Planck EMC WG meeting, H-P-ASPI-MN-811, 17/01/2002
[WG-14] EMC/Power WG meeting #14, H-P-ASPI-MN-1360, 23/04/2002
[WG-HFI] HFI EMC meeting, H-P-ASPI-MN-1361, 24/04/2002

2.2.4 Grounding diagrams documents

[GND-1] Herschel grounding diagrams, H-P-2-ASPI-TN-0199
[GND-2] Planck grounding diagrams, H-P-3-ASPI-TN-0200
[GND-PACS] PACS System Grounding Diagrams, PACS-ME-LI-006, issue 1, 19/02/2001

2.2.5 EMC test reports

[TR-1] Preliminary EMC measurements to determine the E-field at and inside the HIFI Mixer Sub-Assembly, SRON-U/FPU/TR/2001-001, 10/04/2001
[TR-2] Dummy mixer sub-assembly EMC test, SRON-U/FPU/TR/2001-002, draft, 18/07/2001
[TR-3] Radiated E-field susceptibility of various FPU components, SRON-U/FPU/RP/2002-001, issue 1, 20/02/2002

2.2.6 Frequency plans

- Herschel/Planck frequency plans, H-P-1-ASPI-PL-0201
- PACS EMC Control Plan & Frequency Plan, PACS-ME-PL-015, Draft 0.2, 14-01-02

3. CS/CE ON PRIMARY POWER LINES

3.1 Steady state

A rough analysis was carried out in order to show that an intrinsic CS/CE margin exists between the specifications.

The CE DM specification of a unit consuming 1A was increased of 10Log60, considering a satellite consuming 60 A (worst case) and a statistical combination of unit CE (10Log(I) in stead of 20Log(I) variation law).

Then this value vas multiplied by the LISN impedance in order to get a rough idea of the voltage ripple at power bus star point.

Of course this approach is not fully valid, especially at high frequency, but it is a worst case as it doesn't take into account the decoupling between different PCDU power outputs.

Anyway, it allows to demonstrate a minimum CS/CE margin in differential mode between 26 and 32 dB, meaning that the CE and CS specifications are consistent (cf. following figure).

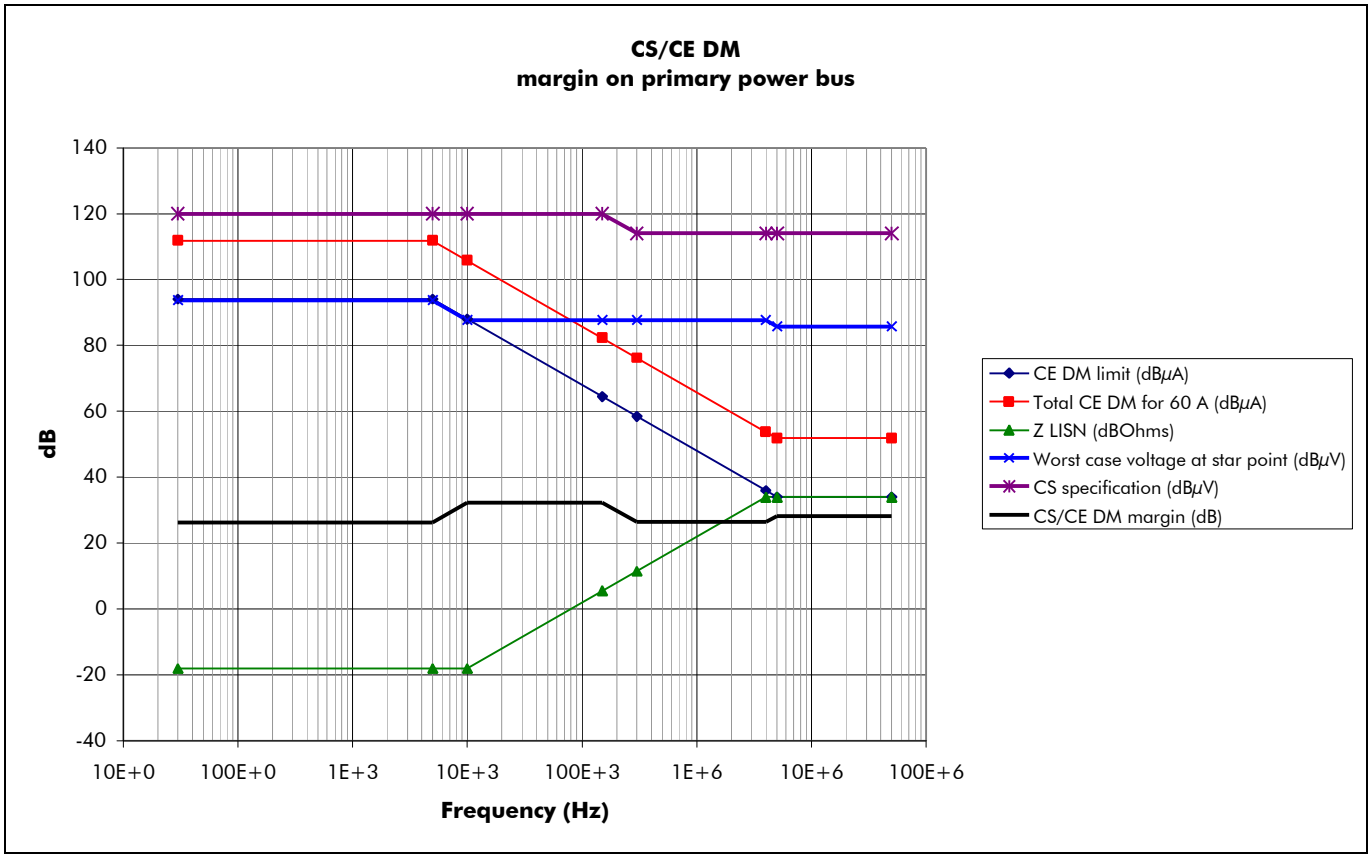

3.2 Transients

3.2.1 Differential mode

The following figure compares the PCDU step load transient mask and the voltage CS transient mask defined in the EMC specification.

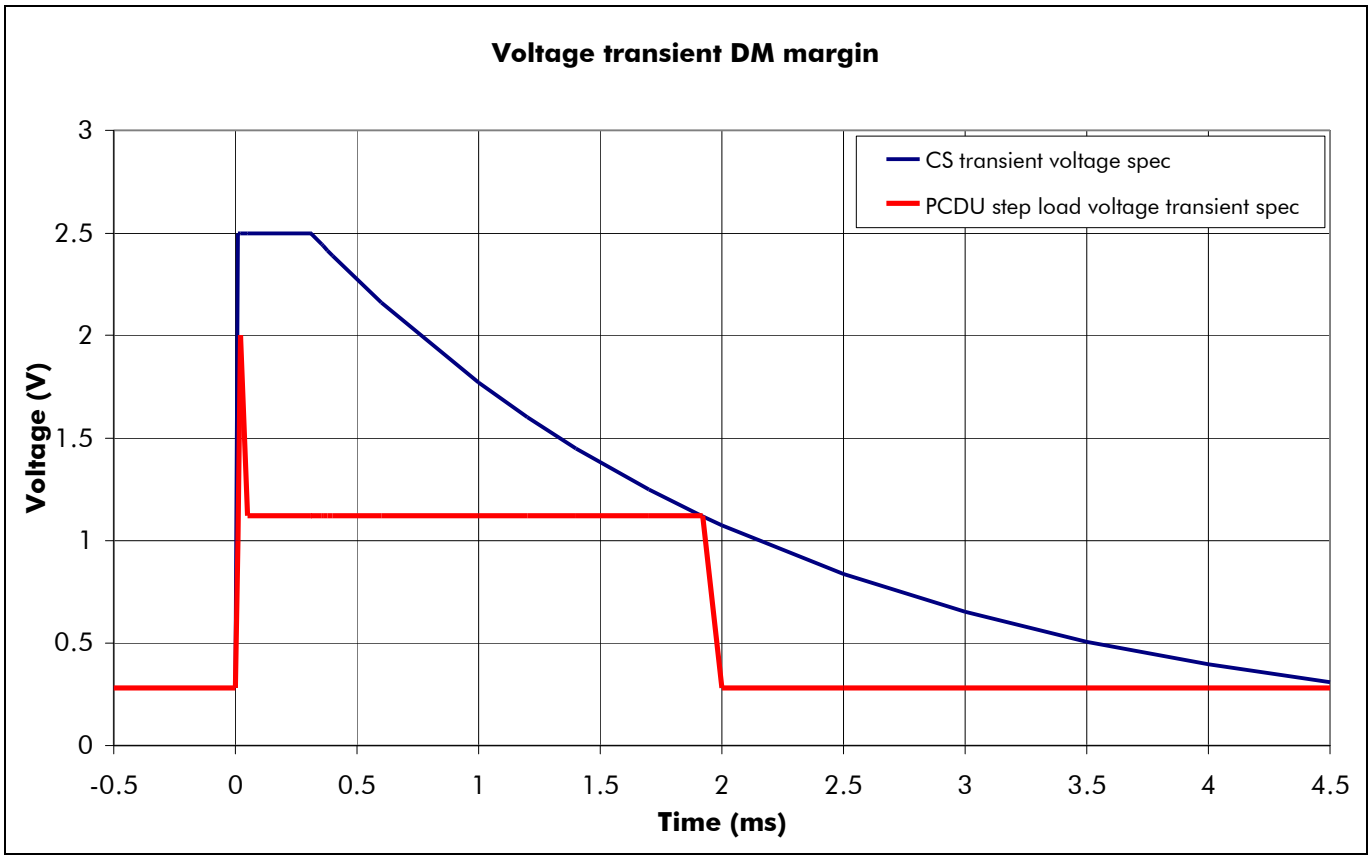

The margin between the corresponding energy levels (or $S(V^2*dt)$) is about 6 dB.

3.2.2 Common mode

A note was written evaluating the common mode voltage transient liable to be created between return and chassis at a unit 28V power interface by a short circuit failure of another unit, order to justify the common mode CS transient specification.

Two kinds of short circuits were considered :

- hot wire to return
- hot wire to chassis

This note is in Annex 1 of the present document.

The EMC spec requires to measure such transients in the frame of the PCDU qualification, that should be lower than 14 V / 2.5 μs (Requirement EMCPCDU-070).
The test set-up would be the following :

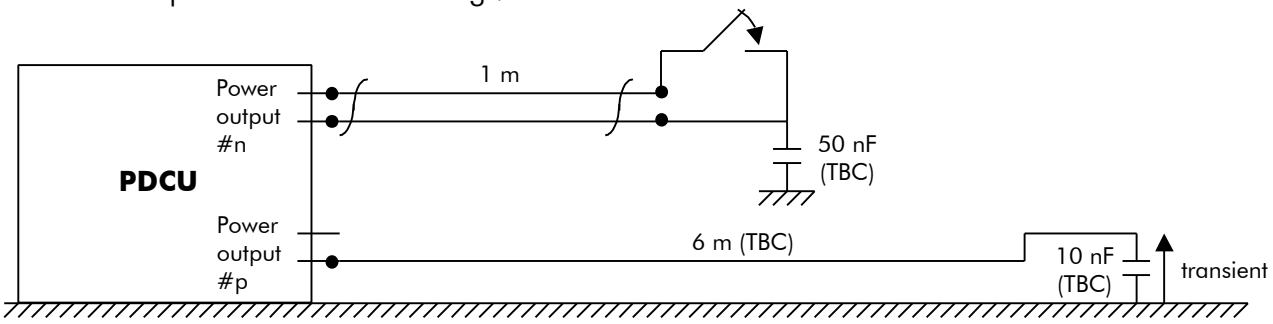

A common mode CS transient ("CS06" shape, 28 V, 10 μs) is specified to all the users of the powers bus (Requirements EMCEQ-570 and followings) :

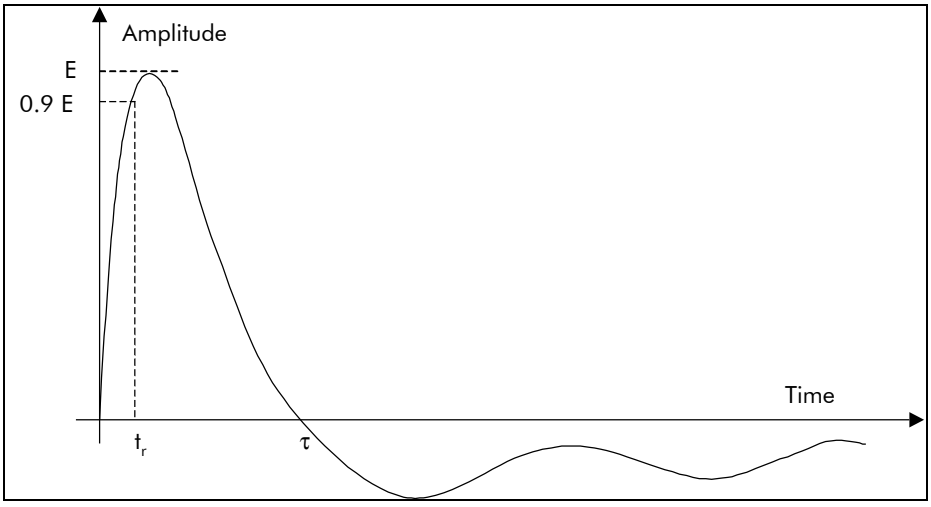

The margin between the two above mentioned specifications is about **12 dB**.

4. RF COMPATIBILITY ANALYSES

4.1 Spacecraft's self-compatibility

4.1.1 Instruments RF compatibility with the Spacecraft's TTC Rx

The field level corresponding to the RF telecommand from earth can be computed using $P_R = \frac{E^2}{120\pi} \times G_R \times \frac{\lambda^2}{4\pi}$ as follows :

Rx nominal power at diplexer (dBm)	-130
Worst case Rx antenna gain (dBi)	-3
Frequency (Hz)	7.208E+9
Wavelength (m)	41.6E-3
Corresponding minimum incident field level from ground (dBμV/m)	27.37

A C/I of about 30 dBc is needed with respect to any interference spectrum line, so the RE requirement in the Spacecraft's TC band was changed for 0 dBμV/m.

From the Instruments frequency plans, it appears that all of them but one use only low frequency electronics that would comply with this requirement.

HIFI design is the one that involves the highest frequency clocks and local oscillators.

HRH/HRV ACS clock (550 MHz) 13th harmonic frequency is 7.15 GHz, which is out of the spacecraft TC frequency band.
HRI 1.25 GHz local oscillator 6th harmonic frequency is 7.5 GHz, which is also out of the spacecraft TC frequency band.

The problem may be the WEH/WEV comb oscillator (100 MHz) with a maximum power level of 23 dBm, the 72th harmonic of which is 7.2 GHz which is just 7.8 MHz away from the X-band uplink frequency that is 7207.8483 MHz.

HIFI IID-B's 2.0 and 2.1 mention that "the comb oscillator generates strong harmonics in the X-band", but it is not quantified.

So HIFI compatibility with the TTC Rx remains to be assessed on the basis of HIFI future information.

4.1.2 Herschel RF self compatibility

4.1.2.1 HIFI RF compatibility with the rest of Herschel Spacecraft in IF band

4.1.2.1.1 HIFI spectrometers radiated susceptibility

At the time of the SRR, HIFI radiated susceptibility drivers in the IF band [3.5 – 9 GHz] were supposed to be the spectrometers (HRS, WBS), with a shielding efficiency between 80 and 90 dB.
The compatibility with the TTC X-band emission seemed then possible to reach to ASPI, from on an analysis partially reproduced hereafter based on the so-called "oversized cavity theory".

4.1.2.1.1.1 Expectable RE from the TWTA at the transmission frequency

RE tests performed on a 115W X-band TWTA on a telecom program gave 89.4 dBμV/m at 1m at 7.5 GHz at saturation.
Considering 30W for Herschel TWTA, 84 dBμV/m can be expected, meaning that the RE specification (69 dBμV/m) is challenging for the tube.

4.1.2.1.1.2 Oversized cavity theory

At 8 GHz, the SVM behaviour should be modelled as a multimode - or oversized - cavity, intermediate between those of a free space and of a resonant cavity.
According to this theory, the ambient fields in the cavity are roughly homogenous and isotropic. The distance between units is not a relevant parameter, and the orientation and polarisation of a given leaking point does not matter.
A given amount of RF power injected into the cavity is uniformly attenuated ; the power picked up by a receive probe is independent of the probe location and orientation.
This fixed attenuation is called cavity insertion loss X_c. It is a function of the area of the apertures, wall conductivity and magnetic permeability, and of the frequency.

The cavity insertion loss X_c is a combination of a radiative component X_ρ (corresponding to the power radiated through the apertures and slots) and a conductive component X_σ (corresponding to the ohmic losses in the walls).

$$\frac{1}{X_c} = \frac{1}{X_\rho} + \frac{1}{X_\sigma} \text{ with } \frac{1}{X_\rho} = \frac{8\pi S_0}{\lambda^2} \text{ and } \frac{1}{X_\sigma} = \frac{8\pi(S - S_0)}{\lambda^2}\sqrt{\frac{\pi}{\lambda C \sigma \mu}}$$

Where S is the overall area and S_0 the total surface of apertures and slots.

The spurious power radiated by the TWTA at the X-band TM frequency is equal to :

$P_r = \frac{E_r^{\,2}}{30}$ with E_r the RE field measured in free-space in the standard conditions of test at 1 m.

In the SVM oversized cavity, the spurious radiated power P_r suffers an attenuation equal to the cavity insertion loss X_c, that becoming $P_r' = X_c.P_r$

And the corresponding spurious field at any point of the SVM cavity is :

$$E_r' = \frac{4\pi}{\lambda}\sqrt{30.P_r'}$$

4.1.2.1.1.3 Application of the oversized cavity theory to Herschel SVM at X-band TM frequency

Considering a typical value for X_c of –30 dB, we obtain the following :

For E_r = 84 dBμV/m :
P_r = -20 dBm, P_r' = -50 dBm (10 nW) and E_r' = 180 mV/m (105 dBμV/m).

With a shielding efficiency of the spectrometers SE = 90 dB, the corresponding EMI level would be –140 dBm at 8 GHz.

Such an EMI pick-up level may have been acceptable for HIFI.

4.1.2.1.2 HIFI FPU in-band radiated susceptibility

Anyway, since the SRR, from analyses and tests performed by B.J. van Leeuwen and P.J. de Groene from SRON [TR-1], it has appeared that the FPU itself is the susceptibility driver.

A RS relaxation from 2 V/m to 2 mV/m was requested by SRON in the IF band, although not formally up to now, and was informally agreed by ASPI.

It was shown in analyses like [AN-1] that one could not expect any cryostat shielding efficiency above ~ 1 GHz.
It was also explained that the cryostat shielding efficiency was not the perfect tool to express the radiated coupling between SVM units and HIFI FPU, as at the frequencies of interest, [3.5 – 9 GHz], the radiation patterns have a significant impact : big objects such as the SVM or the cryostat certainly don't have an omnidirectional behaviour.

In [AN-4] it is concluded that the interference in the 4-8 GHz band should be less than –155 dBm at the output of the mixer unit.

In [TR-3], the maximum allowable interference signal level of the various FPU RF sub-units in the 4-8 GHz band is defined so that this –155 dBm EMI level can be met with a 2 mV/m EMI field level instead of 2 V/m.

These maximum allowable interference signal levels are reproduced in the following table, and the corresponding shielding efficiency values and antenna factor values are calculated.

	Frequency (GHz)	Field level (V/m)	Allowable "average max" interference signal level (dBm)	Corresponding min SE (dB)	Corresponding min AF (dBm-1)	Corresponding max 1/AF (m)
Mixer units	6	2	-69	42.3	88.0	4.0E-5
IF1 amplifier input	6	2	-75	48.3	94.0	2.0E-5
Isolators output	6	2	-78	51.3	97.0	1.4E-5
IF2 amplifier input	6	2	-75	48.3	94.0	2.0E-5

Notes :
The S.E. is here defined as 1/G, G being the antenna gain value corresponding to the power pick-up of interest, i.e. :

$$SE(dB) = -P_{EMI}(dBm) + E_{RS}(dB\mu V/m) + 10 \cdot \log\frac{\lambda^2}{4\pi} - 115.76$$

The antenna factor AF is here defined as E_{RS}/V_{EMI} across 50 Ω.
Across 50 Ω, P(dBm) = V(dBμV) –107, so we have :

$$AF\left(dBm^{-1}\right) = -P_{EMI}(dBm) + E_{RS}\left(dB\mu V/m\right) - 107$$

From [TR-3], two of the 6 Mixers Units (MU4 and MU5) don't meet their SE goal of ~ 42 dB (15 to 20 dB are missing).

On top of the mixers SE, to meet the [AN-4] –155 dBm interference requirement at the output of the mixer unit with 2mV/m radiated interference level, 26 more dB of SE are needed.

So far, the SE of the MSA (Mixers Sub-Assembly) is evaluated by SRON to 5 dB, meaning that the MSA SE needs to be improved by 21 dB. This will certainly not be straightforward as the MSA shielding efficiency is limited by the entrance aperture where the sub-mm beam enters the box, the cut-off frequency of which is about 4 GHz.

On the spurious emission side, the RE-E spec has been updated to include a large notch in the 3.5 – 9 GHz band with a level of 15 dBμV/m.

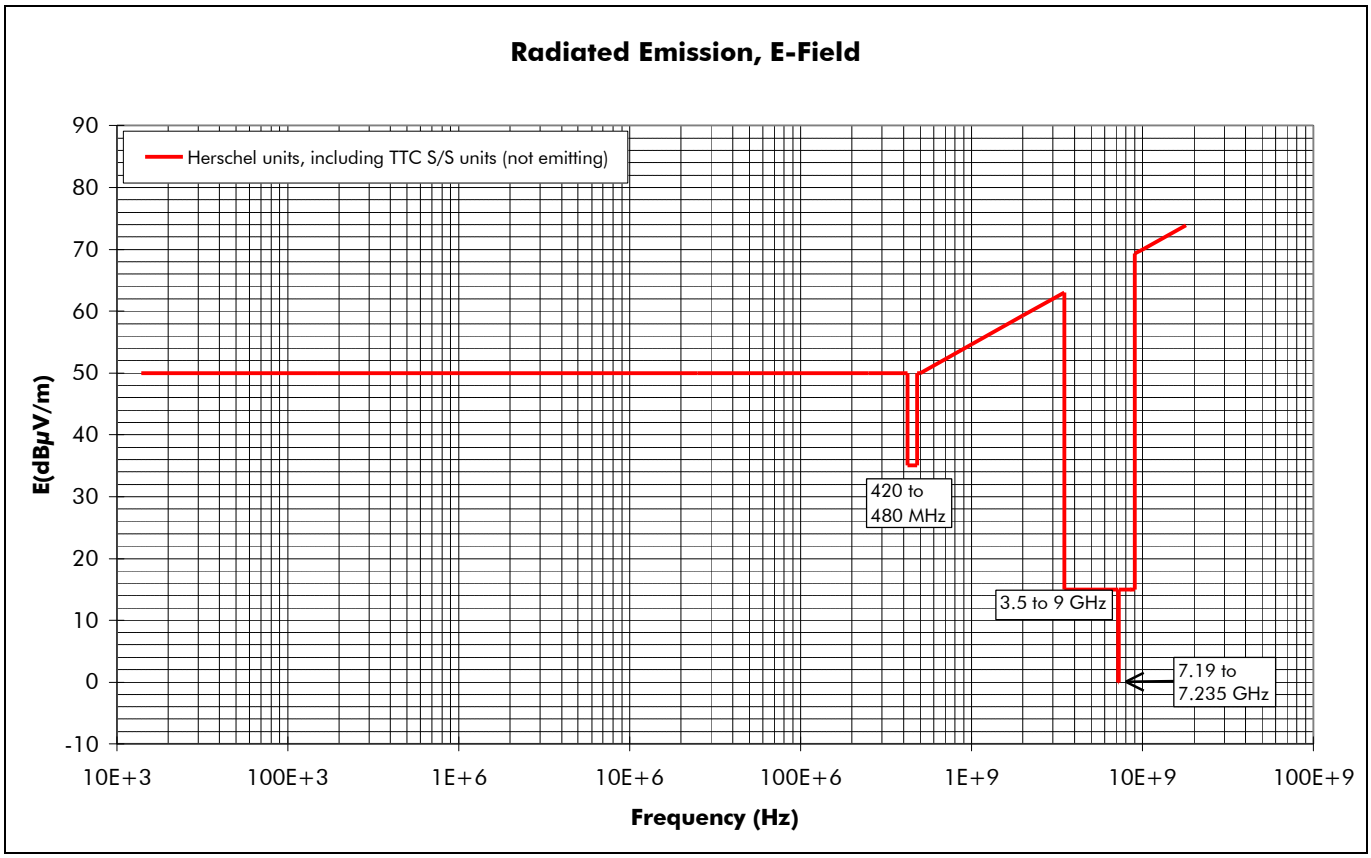

One SVM unit in particular that was expected to be liable to be non compliant with the RE specification in the [3.5 – 9 GHz] notch that is the X-band transponder receive part.
However, Alcatel Espacio has announced no out of specification, so we will assume its RE is 15 dBμV/m.

As a first approach we will consider no shielding efficiency at all for the SVM structure and the cryostat structure (this point will be discussed in the next paragraphs), and 6 dB free space losses.

The system margin is then calculated with various hypotheses in the following table :

SE MU	SE MSA	Total SE	Rx TTC radiated emission at 1m	Free space losses (dB)	Interference field at PLM level (dBμV/m)	EMI level (dBm)	System margin (dB)	Comment
25	5	30	15	6	9	-173.8	18.8	Worst case assumptions
42	5	47	15	6	9	-190.8	35.8	Optimistic
42	26	68	15	6	9	-211.8	56.8	Very optimistic

There may be some unknown positive margin resources in the RF decoupling between a unit inside the SVM and the Optical Bench inside the cryostat.

This point is mentioned in [AN-1] :
"The cryostat opening shielding efficiency approach is potentially rather pessimistic as it considers a plane wave with orthogonal incidence. The potential sources of EMI above 1 GHz (where SE drops to zero dB) are in the SVM that is set under the cryostat."

Indeed, beyond the simple shielding efficiency considered with respect to a plane wave with orthogonal incidence, some more RF decoupling will be brought by shadowing effects.

As suggested in [AN-1] a solution to assess the unknown extra positive margin would be to perform either a GTD or a MoM analysis in order to compute the coupling between a spurious RF source in the SVM and the optical bench, through the CVV "cavity" and cryostat openings.

However this "extra" margin calculation should be used only in the last resort as it would rely on a tricky analysis exercise.

In the end, one can expect with reasonable assumptions a ~ +20 dB margin with worst case assumptions, as long as the spacecraft X-band receiver is compliant with its RE specification.

Note :

HIFI LO subsystem LSU unit as well would be liable to radiate significant spurious levels in the IF band, as it incorporates four oscillators operating in or adjacent to the HIFI IF band with a maximum power level of +24 dBm.
HIFI system assessment [AN-4] is that the 114 dB shielding effectiveness necessary to achieve a RE E-field limit of 15 dBμV/m at 1 m should be achievable "with careful design and the proposed double shielded construction".

Also, the IF processor of the WBS contains 3 oscillators within the IF band with power levels of +13 dBm, making a 103 dB shielding efficiency necessary to achieve a RE E-field limit of 15 dBμV/m at 1 m.

This is considered achievable by HIFI, "with careful design and the proposed double shielded construction" [AN-4].

So **HIFI Instrument self compatibility, more than the compatibility with the SVM, involves a particularly careful control of the shielding efficiencies on both cold and warm sides.**

4.1.2.1.3 HIFI FPU out-of-band radiated susceptibility (1 to 4 GHz)

At the EMC meeting [WG-14], HIFI explained that their mixers are expected to be sensitive in the 1-4 GHz band (interference via harmonic generation into the IF band).

They are expecting to need a RS relaxation in this band as well, that is to say that the general RS spec relaxation would have the following shape :

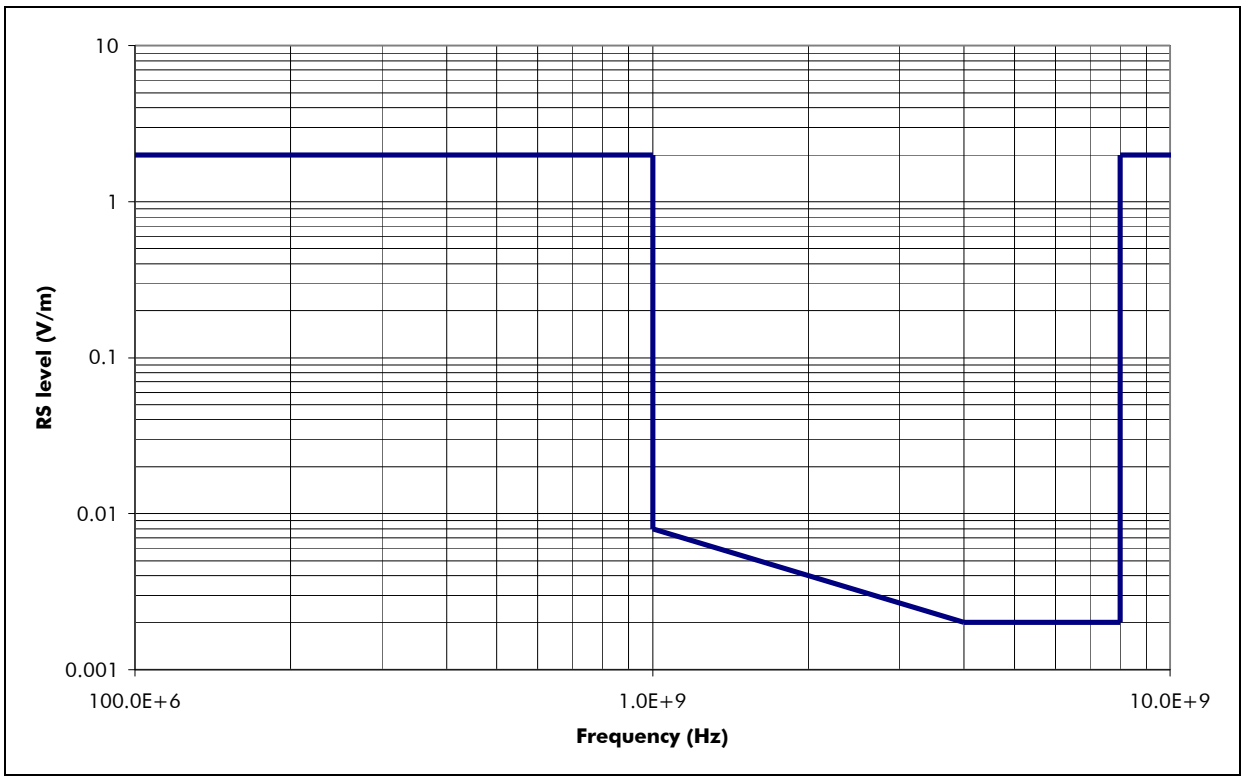

A CR is expected from HIFI to formalise this.

This would then involve a significant RE specification modification to keep guaranteeing a comfortable system margin.

4.1.3 Planck RF self compatibility

4.1.3.1 LFI RF compatibility with the rest of Planck Spacecraft

One major point concerning Planck satellite self compatibility is the coupling between the TTC antenna and the Planck detectors. : During scientific observation, data telemetry is nominally performed using the Medium Gain Antenna (MGA). It can also be envisaged to perform low rate data transmission using the Low Gain Antenna (LGA). For both antenna, a preliminary analysis has been carried out to estimate the observation signal to interference ratio, that is summarised hereafter.

Both LGA and MGA are implemented on the solar array oriented toward the earth.
The aim is to compute the power level of the TTC reaching the detectors in the focal plane. The worst case analysis consists in performing the analysis for the detector working at the lowest frequency (LFI 27 at 30 GHz). This power has to be compared to the observation signal power.
The computation of the observation signal power is performed by computing the integrated black body luminance Φ [T].

$$\varphi [\nu,T] = (2.h/c^2)\ \nu^3 / (\exp[h.\nu/k.T]-1)$$

$$\Phi [T] = \int_{BW} \varphi [\nu,T]\, d\nu \approx 1/4\ (\ \varphi [\nu_{min},T] + 2\ \varphi [\nu_c,T] + \varphi [\nu_{max},T]\ ) * (\nu_{max}-\nu_{min})$$

The black body luminance is multiplied by the primary mirror surface and by the telescope solid angle. This solid angle is obtained knowing the telescope on axis-directivity at 30 GHz using : $\Omega=4*\pi$ / Directivity.

Hence the power of the observed signal is :

$$DC_{power}=\Phi [T=2.7K] * \Omega * Mirror\_surface$$
$$DC_{power}=-91.22\ dBm$$

The required sensitivity is 2E-6 leading to temperature deviation of 5 μK.

Hence the power variation of the observed signal is :

$$AC_{power}=(\Phi[T_{max}]-\Phi[T_{min}]) * \Omega * Mirror\_surface$$
$$AC_{power}=-147.10\ dBm$$

Then the parasitic signal coming from the TTC antenna has to be compared to the AC_{power} level.
The following table provides the numerical details for this power computation.

Integrated luminance over 27 GHz – 33 GHz	Φ (W/sr/m²)	3,40E-09
Luminance deviation	$\Delta\Phi$ (W/sr/m²)	8,78812E-15
Primary surface	(m²)	1,77
Solid angle	(sr)	0,000125664
AC power	(W)	1,9547E-18
AC power	(dBW)	-177,1
AC power	(dBm)	**-147,1**
DC power	(W)	7,55873E-13
DC power	(dBW)	-121,2
DC power	(dBm)	**-91,2**

The second phase of the analysis is to perform the link budget between the TTC antenna and the detector LFI 27. This is done using the standard formula :

$$P_r = P_e * G_e * L_{FS} * G_r$$

P_e : TTC output power in X band attenuated by 30 dB for the harmonic at 30 GHz.
G_e : TTC antenna gain
L_{FS} : free space losses $L_{FS} = (4*\pi*R / \lambda)^2$
G_r : gain of LFI 27 detector or, more precisely, coupling factor toward the TTC antenna.

The coupling factor between the horn LFI 27 and the TTC antenna was computed using grasp8 multi GTD. The ray combination is : diffraction on baffle edge then diffraction on the 3 cascaded grooves to finally diffract at the edge of the solar array. This ray combination is displayed on the following figure.
A gain of –145 dBi is found.

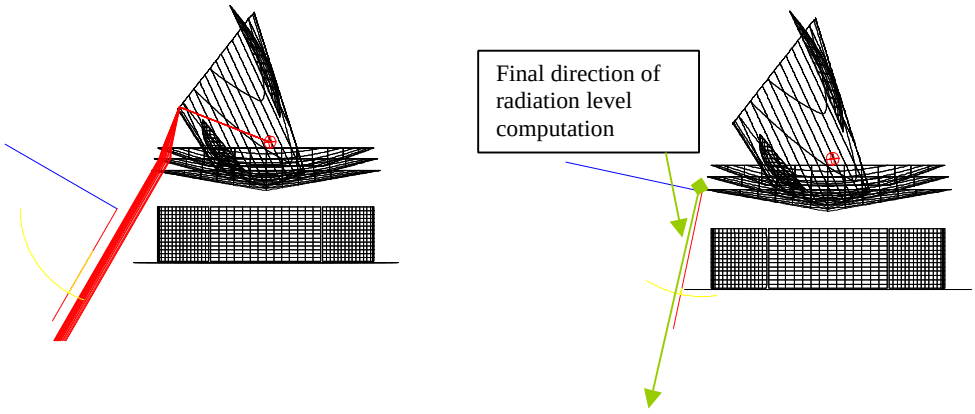

A worst case link budget is displayed in the following table. The 3 dB antenna gain is a worst case which envelopes both LGA and MGA gains at 90 deg from their axis. The TTC spurious signal reaching the LFI27 detector is 57 dB below the observed signal.

X band TTC antenna output power (W)	30
X band TTC antenna output power (dBW)	14.77
Out of band level attenuation (dB)	30 (typical conservative value)
TTC antenna output power at 30 GHz (dBW)	-15.23
LFI 27 horn reception gain (dBi)	-145
Frequency (GHz)	30
Wavelength (m)	0.01
Distance between LFI 27 horn and TTC antenna (m)	6.10
Free space losses (dB)	-77.69
TTC antenna transmit gain (dBi)	3.0
Received power (dBW)	-234.92
Received power (dBm)	-204.92
CMB AC level (dBm)	-147.1
Observation signal to interference ratio (dB)	**57.8**

The result of this analysis is that TTC antennas do not interfere with the mission with large margins.

The tests foreseen on the RFDM (Radio Frequency Development Model) and RFQM (Radio Frequency Qualification Model) will allow to check the validity of the computation methods used to determine the radiation pattern over 4π steradian (GRASP8 validation).

4.2 Spacecraft compatibility with launcher

The RE and RS specifications relative to Ariane 5 and to the CSG launch site are recalled hereafter :

RE-E :

35 dBµV/m [420 MHz - 480 MHz] (launcher TC)
70 dBµV/m [5.45 GHz - 5.825 GHz]

RS-E :

Overall level : 0.1 V/m, i.e. 100 dBµV/m
18 V/m [1.0 - 1.5 GHz], i.e. 145 dBµV/m
18 V/m [2.2 - 2.29 GHz], i.e. 145 dBµV/m (launcher TM)
18 V/m [2.9 - 3.4 GHz], i.e. 145 dBµV/m
18 V/m [5.4 - 5.9 GHz], i.e. 145 dBµV/m (launcher/ground radar)

During launch phase, of the RF units, only nominal and redundant TC receivers are ON.

4.2.1 Spacecraft RE / Launcher RS

4.2.1.1 Spacecraft Telemetry transmission

On the launch pad, the Spacecraft 30 W X-band telemetry transmission is supposed to be off.
No compatibility problem with the launcher related to the Spacecraft telemetry transmission is to be taken into account.

4.2.1.2 Spacecraft spurious emission in launcher TC band

The RE from the spacecraft in launch mode in the launcher [420 – 480 MHz] destruction band will be driven by the spurious emission from the CDMU and its harness.

The experience from previous programs lets us expect that the spacecraft should be compliant with the 35 dBµV/m Ariane requirement with roughly 20 dB margin.

In their "Statement of compliance to technical applicable document", P-HPL-SOC-0005-SE, 16/10/2001, SAAB stated that "measurements on earlier similar units indicate that the requirement on 420-480 MHz will be hard to fulfil".

However ASPI position remains that with a distributed grounding strategy of the CDMU digital 0V layers and taking into account some spacecraft structure shielding effect, the Ariane requirement is expected to be fulfilled.

4.2.2 Launcher RE / Spacecraft RS

The only satellite RF units which may be perturbed by the launcher RE are the 2 X-band TC receivers.

The spurious RF power from the launcher received in band by the TC receivers, and the power received out of band in the various special frequency bands were computed using :

$$P_R = \frac{E^2}{120\pi} \times G_R \times \frac{\lambda^2}{4\pi}$$

Reasonable assumptions were made for the out-of-band antenna gain and the typical X-band diplexer rejection (i.e. the S_{21} parameter).

The spurious power levels received in the 5 considered bands and the margins with respect to the TC receiver overload capability are presented in the following table.

	Launcher spurious RE-E	Launcher TM	Launcher/ ground radar emission	Launch site environment	Launch site environment
Specified radiated level from the **launcher** (dBμV/m)	100	145	145	145	145
Specified radiated level from the **launcher** (V/m)	0.1	17.8	17.8	17.8	17.8
Frequency (Hz)	7.2E+9	2.2E+9	5.4E+9	1.0E+9	2.9E+9
Wavelength (m)	42.E-3	136.E-3	56.E-3	300.E-3	103.E-3
Worst case **S/C** TTC antenna gain (dBi)	6	0	0	0	0
Worst case **S/C** TTC antenna gain (linear)	2.0	1	1	1	1
S/C TTC input losses + diplexer rejection (dB)	2	20	10	20	20
Maximum power at **S/C** TC receiver input (dBm)	-53	-19	-17	-12	-21
S/C TC receiver overload capability (dBm)	0	0	0	0	0
Margin (dB)	**53**	**19**	**17**	**12**	**21**

The diplexer rejection figures are TBC but we can already establish **that with worst case assumptions we have positive margins in all cases**.

If the diplexer rejection values taken into account happen to be optimistic, the analyses will be refined in order to consolidate the margins (by considering more realistic antenna gain and input losses values).

5. INSTRUMENTS DETECTION CHAINS PROTECTION AGAINST EMI

5.1 Instruments noise specifications / noise rejection concepts

5.1.1 SPIRE

The figure next page, reproduced from SPIRE design description document, SPIRE-RAL-PRJ-000620 , issue 1.0, 04/02/2002, shows a schematic representation of the SPIRE signal chain with noise sources, gains, and impedances through the system.

A few relevant extracts of the same document are reproduced hereafter :

- "The bolometers are excited by an AC bias at a frequency of approximately 100 Hz, which eliminates 1/f noise from the JFETs, giving a 1/f knee for the system of less than 100 mHz"
- "The impedances of the NTD bolometer elements are on the order of 5 MOhms. This represents a compromise between high responsivity (which requires high impedance) and immunity to EMI and microphonic disturbance, which require a lower impedance). The JFETs located outside the FPU convert the impedance of the detection circuit to approximately 7 kOhms"

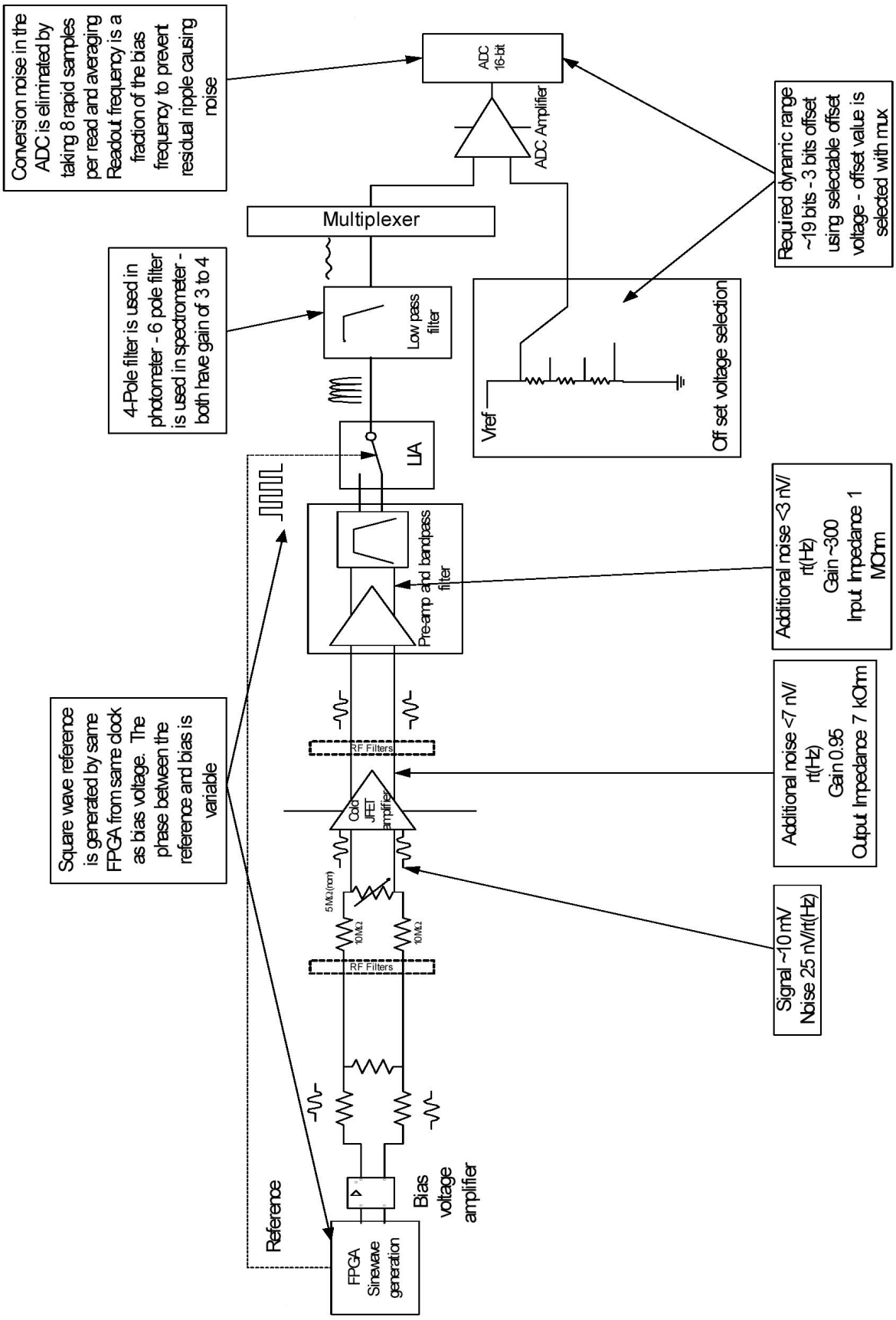

5.1.2 PACS

5.1.2.1 PACS bolometers

The impedance levels along PACS bolometers analogue detection channels are optimised to provide the necessary bandwidth while favouring EMI rejection as far as possible.

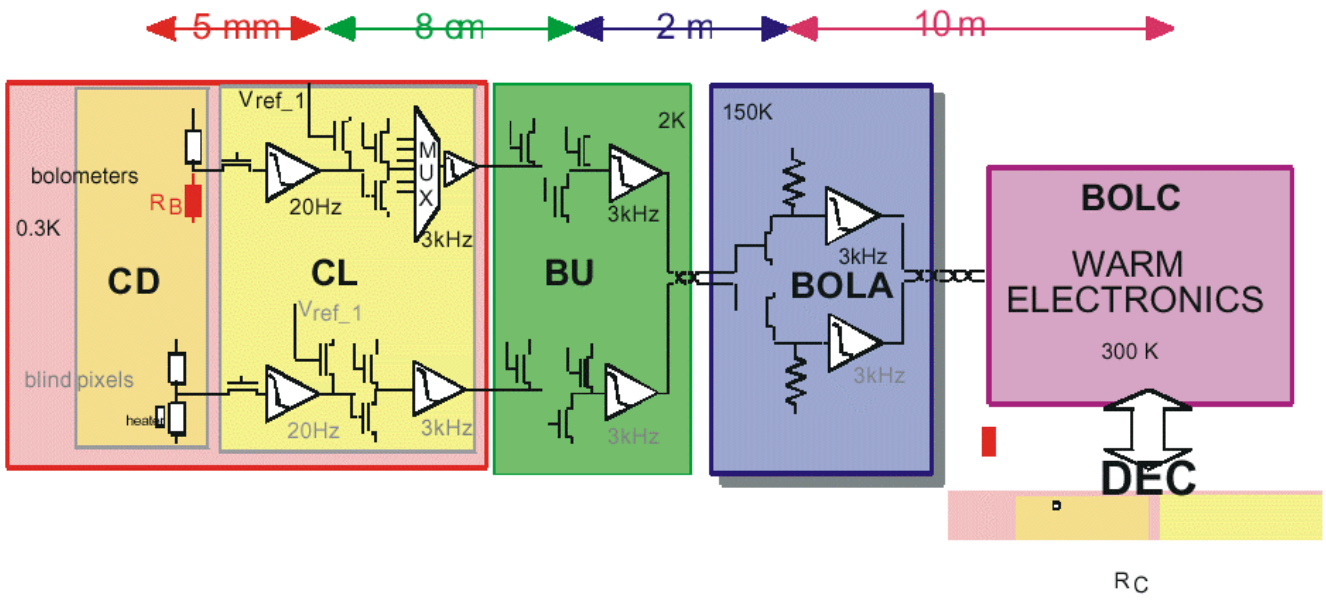

Schematics of the cascaded impedance adaptation readout circuits –
Reproduced from PACS Instrument Desciption Document, PACS-ME-GR-002, part II, 28/01/2002
CL stands for "Circuit de Lecture".

According to PACS documentation "the detector resistance bridge itself is a very high impedance component to obtain large signal levels (few GΩ)".

Then each stage output impedance together with the harness stray capacitance and the next stage input parasitic capacitance forms a parasitic low pass RC filter, the cut-off frequency of which is shown on the here above figure.

The output impedance decreases from stage to stage, as the harness length increases. Each stage source impedance value is compatible with the following harness capacitive load.

The chain is differential (use of blind pixels) from the detector up to the BOLC. Twisted pair wires are used wherever possible.

An electronic modulation is included just after the bolometer, an before the readout pMOS at 300 mK.
The signal frequency at CL output is then 1280 Hz with a typical amplitude of 100 mVpp.
The signal is the result of a synchronous differentiation (with the blind pixels) and of a time dependant differentiation (with the electronic modulation).

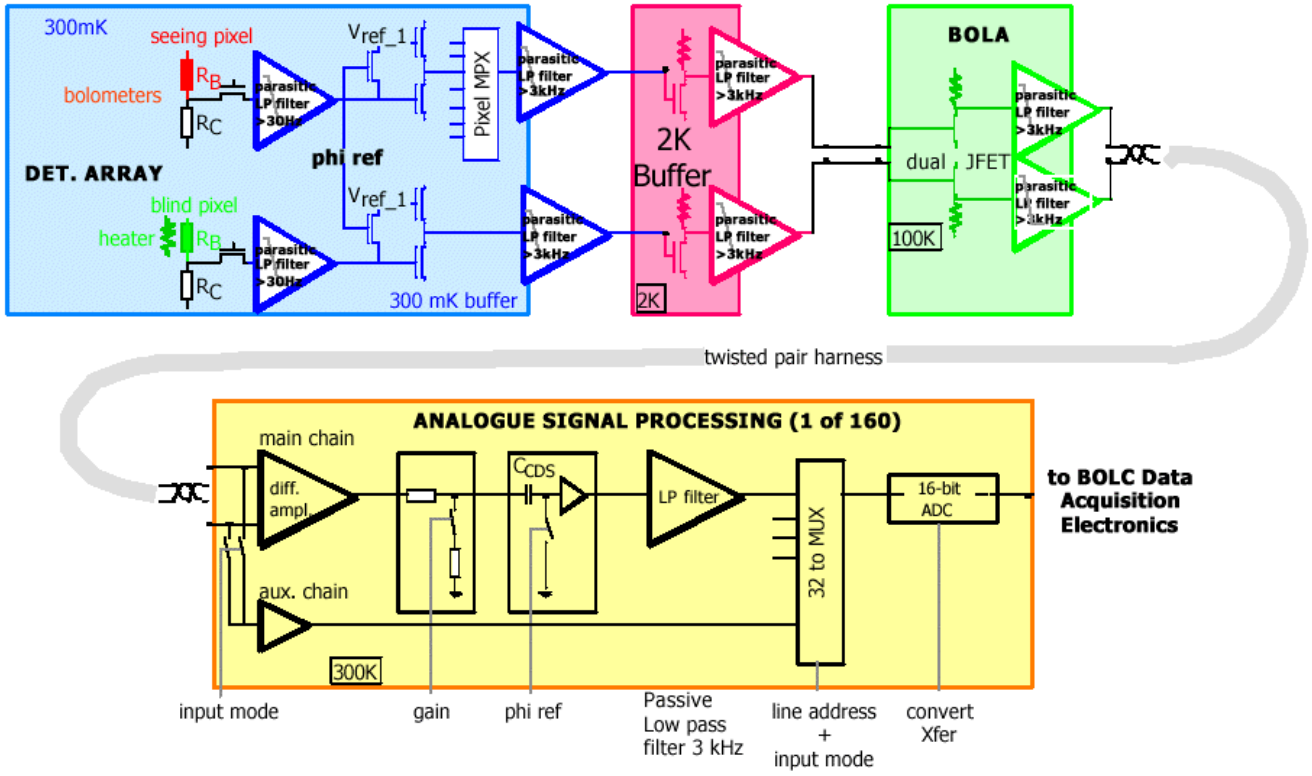

Elementary PACS bolometer analogue channel –
Reproduced from PACS Instrument Desciption Document, PACS-ME-GR-002, part III, 28/01/2002

5.1.2.2 PACS Ge:Ga detectors

The output lines of the Ge-detector modules will carry multiplexed analogue signals with ~ 8 kHz frequency.
For that purpose, triaxial cables are foreseen, with the inner shields driven by amplifiers of gain = 1 in the warm electronics. The concept is to reduce the effective line capacity to nearly zero.

5.1.3 HIFI

The mixers and amplifiers in the FPU are sensitive to noise picked up on their bias lines, as well as to interference within the IF band.

Concerning the mixers, the noise requirements **at the SIS junction** are specified in "SIS Mixer Bias Stability and Noise Requirements", SRON-G/FCU/TN/2000-003, issue 1, 17/07/2000 :

- the bias voltage noise spectral density should not exceed the following limit :

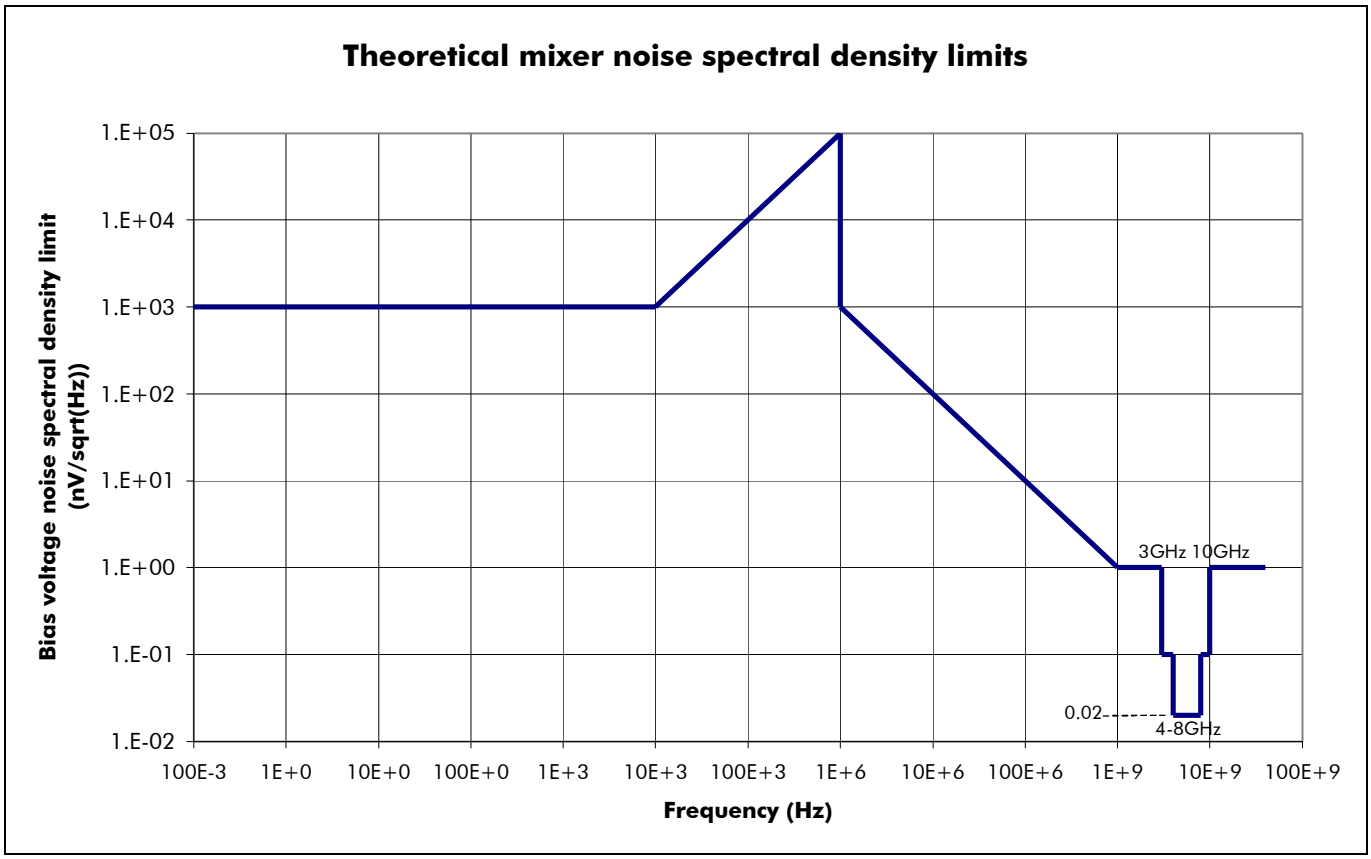

- the total mixer bias voltage noise integrated over the frequency range 0.1 Hz to 4 GHz should not exceed **20 μV_{rms}**.

From the same note : "filtering at the bias circuit in the mixer block, and optionally in the mixer assembly and FPU, will allow significantly higher noise levels in the cryo-harness and the FCU".

From [AN-4], narrowband noise limits can be deduced from the above taking into account the relevant bandwidth for the interference mechanism according to the frequency. "At low frequency, say below ~1 MHz, the interference is detected directly by the chopping sequence and the relevant bandwidth is 1 Hz. At higher frequencies the interference appears in the IF spectrum and effective resolution bandwidth is relevant. The minimum instrument resolution bandwidth for HIFI is ~200 kHz".
The interference limit in band was assessed at **–155 dBm**.
The resulting combined mixer narrowband interference limit in dBm from DC to 40 GHhz is shown on the following figure.

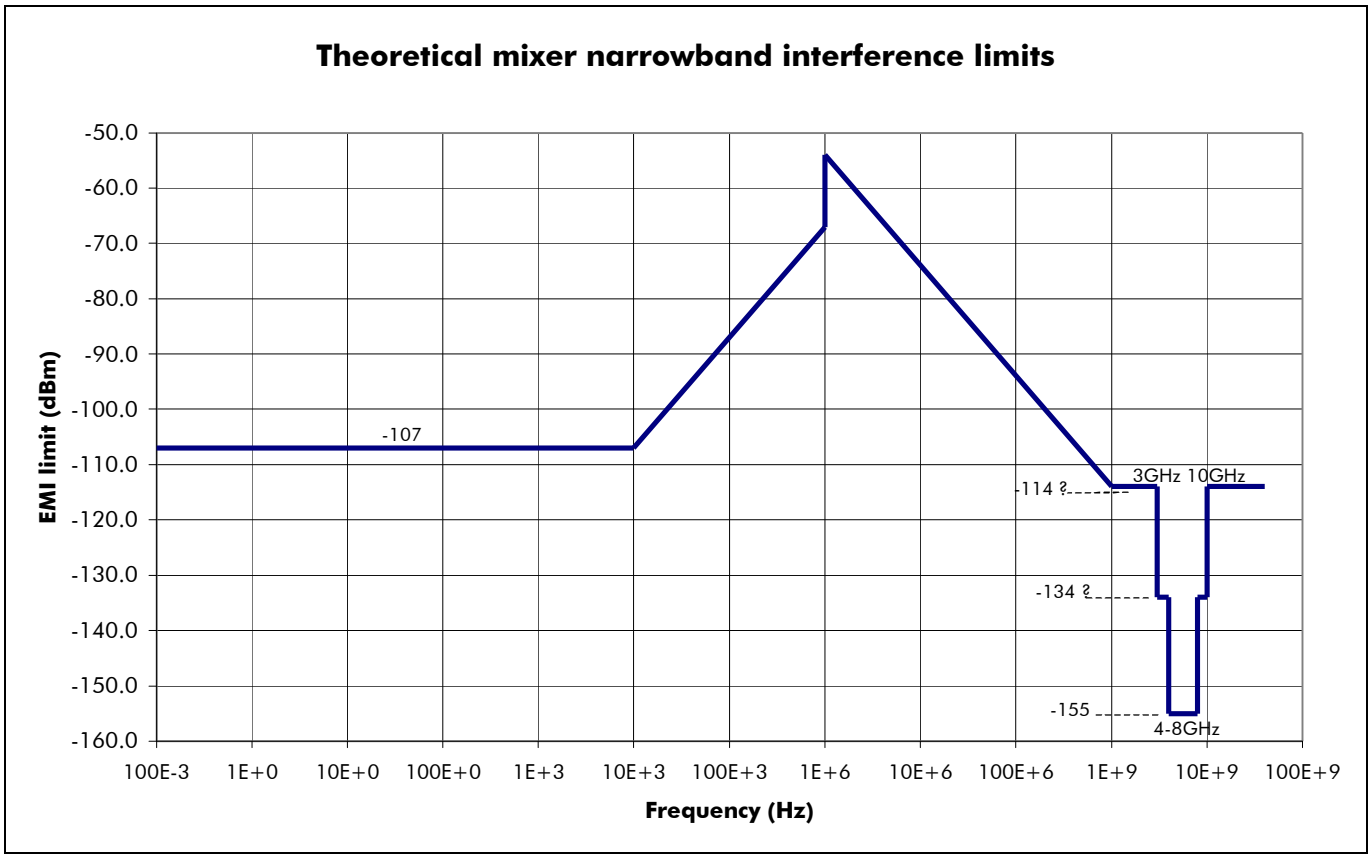

Concerning the IF amplifiers, the requirements for the IF bias signals are based on the demand to assure a sufficient stability of gain (0.1 % in a measurement period).
In [AN-2] they are translated into 0.4 mV_{rms} for the drain-source voltage and 100 μV for the gate-source voltage.

The frequency multipliers and amplifiers in the LOU are also sensitive to noise picked up on their bias lines. The sensitivity of the LOU components to bias noise is discussed in the "LO ESD/EMC Test Plan", JPL/HIFI/PL/2001-001 § 5.1.

Note : from the last pieces of information received from HIFI (22/03/2002), the interference limit in-band (4 – 8 GHz) at the various units is detailed as follows :

Unit	Maximum power level	Interference limit	Notes
FPU	-82 dBm/MHz (nominal)	-155 dBm	IF output to FCU (HRS operational)
FCU	-90 dBm/MHz (nominal)	-125 dBm	IF signal from FPU and to HRI, WEH/WEV (HRS operational)
HRH/HRV (IF processor)	-65 dBm/MHz (nominal) TBD	-127 dBm	IF signal from FCU IF signal internal
WEH/WEV	-90 dBm/MHz -30 dBm/MHz (TBC)	-120 dBm	IF signal from FCU IF signal internal

5.1.4 LFI

The general scheme of each Radiometer Chain Assembly is shown hereafter :

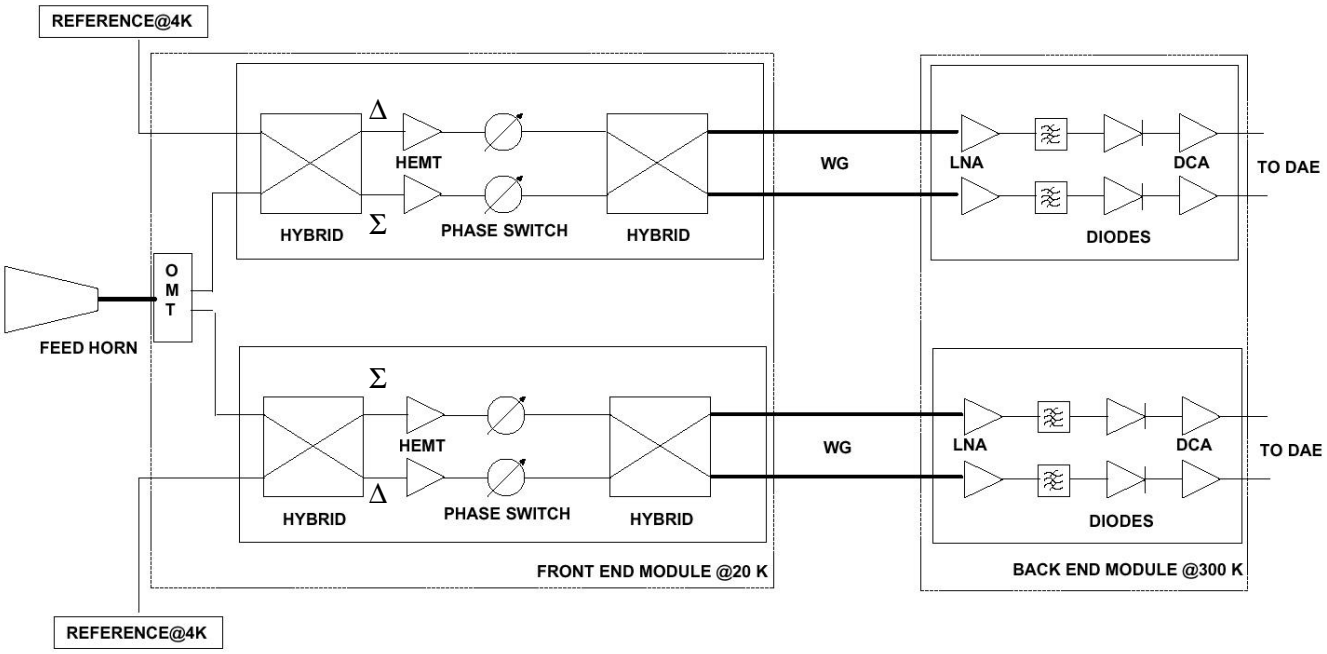

OMT = Ortho Modal Transducer ; HEMT = InP high-electron-mobility transistors
WG = Waveguide ; LNA = Low Noise Amplifier
DCA = DC Amplifier ; DAE = Data Acquisition Electronics

The concept is the following (from LFI design report, PL-LFI-PST-RP-002) :
"The signals from the sky and from a reference load are combined by a hybrid coupler, amplified in two independent amplifier chains, and separated out by another hybrid. The sky and the reference load power canthen be measured and differenced. Since the reference signal has been subject to the same gain variations inthe two amplifier chains as the sky signal, the true sky power can be recovered".

The signal shape at the detector diodes output is the following :

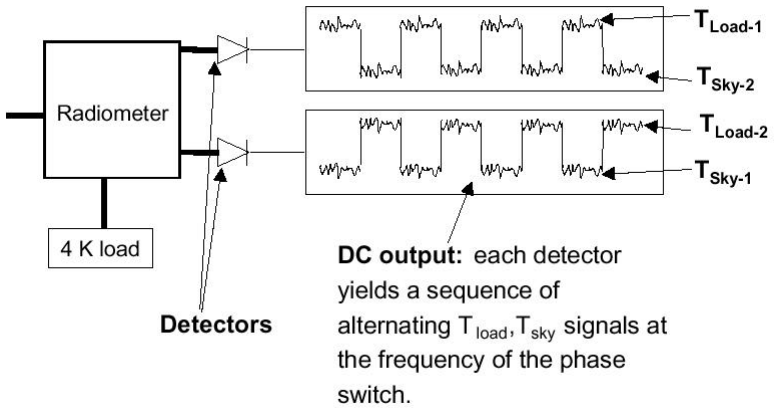

The phase switch and the HEMT gain are controlled by bias lines from the DAE.

From [WG-P1], the maximum spurious noise for the LFI bias lines is **1 μV/**Ö**Hz** and **1 μV** frequency domain integrated in the band.

5.1.5 HFI

HFI uses bolometers detectors. The signal at bolometer level is measured with a noise of a few nanovolts in a circuit with an impedance of several MΩ. The overall noise specification of the readout, given in terms of demodulated signal and including all possible noise contributions from the Readout is 5nV/√Hz from 0.016 Hz to 200 Hz, to be compared with the Jonhson thermal noise of the 0.1 K bolometer resistor that is 5nV/√Hz for 10 MΩ.

The first stage of HFI preamplifier is a JFET pair used as an impedance adapter (input impedance much higher than the detector impedance and output impedance a couple orders of magnitude lower than the detector impedance) and mounted on the 50 K stage as near as possible to the detectors. A follower mounting is used with a gain = 1 (similar to SPIRE design).

The following scheme and table, extracted from "HFI RU System Requirements and Technical Specification", TS-PHCB-100015-CESR, issue 3 rev. 1, 04/01/2002, show an overview of a measurement channel and of the associated signal characteristics and noise levels :

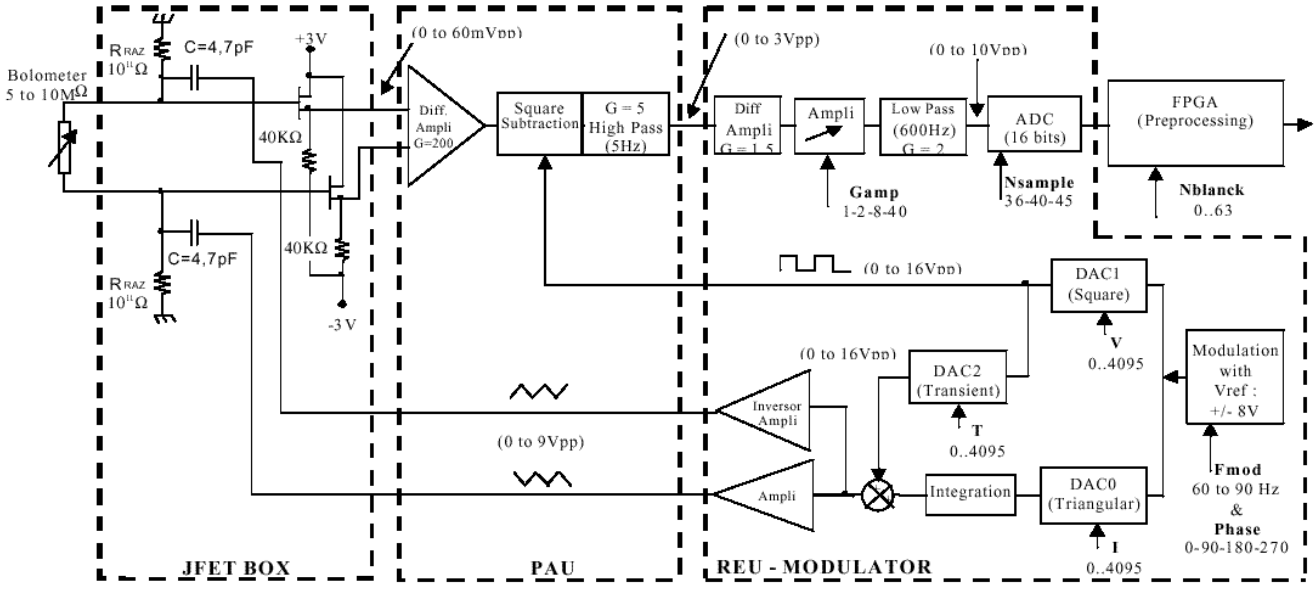

Notice : C = 27pF for thermometer devices

Signal Identification	Amplitude Range	Nominal Range	Noise Level	
JFET-PAU science signal	0 to 60 mVpp	10 mV	10 nV/√Hz	
PAU-REU science signal	0 to 3 Vpp	10 mV	10 μV/√Hz	
ADC science signal	0 to 10 Vpp	400 mV	400 μV/√Hz	
REU square signal	0 to 16 Vpp	1.2 V	100 nV/√Hz from 0.1 Hz to 400 Hz	(contribution to the signal noise less than 1 nV/√Hz)
REU triangular signal	0 to 9 Vpp	0.8 V	20 nV/√Hz from 0.1 Hz to 400 Hz	(contribution to the signal noise less than 1 nV/√Hz)

Detection and bias signals are all differential.
Similarly as SPIRE, a differential AC square bias current (between 70 and 90 Hz) is used to modulate the bolometers signal for FET 1/f noise rejection purpose. It is phase locked with the second harmonic of the driving current of the 4K cooler compressors to reduce frequency beating effects.

5.2 Cryo-harness electrical characteristics

5.2.1 Cryo-harness conductors

From "EMC/ESD analysis report for SDR", ISO.AS.1400.TN.0434, 08/03/89, the resistance of SST gauge 38 wires would be :

- 130 Ω/m outside CVV
- 115 Ω/m inside CVV
- Varying along the link with temperature

Concerning the wires self-inductance, it was stated on ISO that the frequency dependency of μ_r for cryo-harness SST is roughly :

- $\mu_r \sim 200$ for $f \leq 10$ kHz
- $\mu_r \sim 1$ for $f \geq 100$ kHz

And it was concluded that it was useless to take the μ_r into account, as :

- at low frequencies the wires resistance is predominant
- above ~ 1MHz the wires self inductance becomes predominant but $\mu_r = 1$

From the same document (ISO.AS.1400.TN.0434), the following capacitance values were given by the manufacturer :

- 60 pF/m wire to wire
- 100 pF/m wire to shield

5.2.2 Cryo-harness overshieldings

From fax HP-2-ASED-0089/02 "Overall Harness Shield Electrical Characteristics" the ISO outer cryoharness overall shield was constructed of **copper** AWG 36 conductors.

Based on photographs of ISO outer cryoharness overall shields, ASED assume **90% optical coverage**.

On Herschel, there will be about 40 outer cryoharness cable bundles having a diameter from 6 mm to 14 mm and a length between 2.5 and 4.5 m, and according to ASED a 6 mm diameter bundle overall shield would be constructed of about 234 single conductors AWG 36, 1.36 Ω/m each.
The resistance for a bundle bigger than 6 mm diameter would then be less than **6 m**Ω**/m**.

Note : copper overshields were used on ISO only along the Cryostat and on the SVM (cf. figure § 5.5). The portion of the overshield routed on the GF struts between the CVV and the SVM (the part with significant temperature difference) was made of Chomerics "Ferrex" **steel** mesh tape overshield ("shield wrap").
The DC resistance of this portion of the overshiels remains to be assessed by ASED.
It is expected to be significantly higher than the a.m. value, as :

- According to "ISO EMC/ESD analysis report for SDR", ISO-AS-1400-TN-0434, 08/03/1989, the overshield resistance on ISO was 63 mΩ/m, which is one order of magnitude more.
- According to note ISO-TN-B1420.005, 22/04/1988 (information provided by PACS EMC consultant Terence Bax), the DC resistance of a 6 mm bundle overshield would be **155 m**Ω**/m** ± 25%.

5.3 General principles of detection chains protection against EMI

For all the Instruments of both satellites, the main subject of concern is the common mode between SVM and PLM and its coupling to the detection signals due to CM to DM conversion (non infinite CMRR).

The common mode sources may be field to cable coupling (either E or H field) or structure currents flowing in metallic links between SVM, PLM and FPU's. These links (e.g. LFI waveguides and cryogenic piping for Planck ; HIFI coaxial cables, cryogenic piping and harness overshielding for Herschel) will have a conductance limited by thermal constraints and an important total length (> 5 meters).

Among all the EMC susceptibility specifications of IID-A, the main contributor to the common mode noise budget is the requirement 5.14.3.6 "Conducted Susceptibility Common Mode Voltage – Steady State" that specifies 2 V_{pp} between the equipment signal reference and ground plane in the frequency range 50 kHz to 50 MHz.

5.3.1 Protection of sensitive lines against low frequency EMI

5.3.1.1 Grounding strategies against low frequency interference

Analogue 0V lines, such as bias returns, need to be grounded on one end of the detection chain only (either SVM or PLM end) for common mode rejection at low frequency purpose.

However this rejection will decrease with the frequency because of unavoidable parasitic capacitance on the isolated side between isolated return and chassis. This parasitic capacitance will in most cases be bigger between 0V and chassis than between signal "hot lines" and chassis, because, for example of the existence of large analogue 0V layers. But in any case, whatever the design is, there is no way the various parasitic capacitance's can be balanced and this unbalance with result in poor HF common mode rejection, or in other words, common mode to differential mode conversion.

Indeed, we have the following :

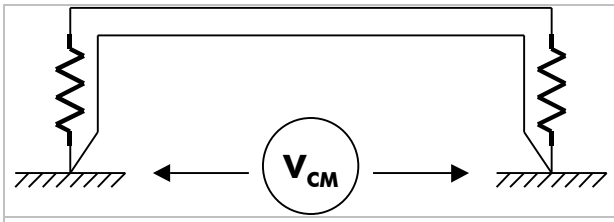	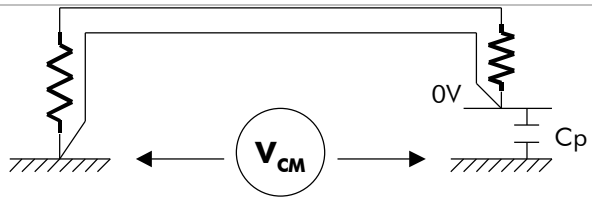
No rejection for F < 10 kHz Slight rejection for F > 10 kHz	Very good CM rejection at low frequency Degenerating like F↗ or like F^2↗ because of the unavoidable parasitic capacitance

In the second case, we have actually a high pass filter, either first order or second order.

As an example, the differential noise induced by a common mode noise source according to frequency for such link of link was computed with PSPICE (cf. PSPICE schematics and plots next page).

The following line parameters were assumed :

- 3 meters
- 100 Ω/m resistance on the "hot" line
- 15 Ω/m resistance on the return line
- L_{diff} = 400 nH/m
- L_{com} = 400 nH/m
- C_{diff} = 30pF/m

… which are arbitrary although not unrealistic for, e.g., HIFI FCU to FPU bias lines.
As an example, the isolated end was adapted and the other end loaded by a big resistance.
However all the possible source & load impedance combinations show more of less the same behaviour or CMRR degradation with frequency.
500 pF were considered for the parasitic capacitance.

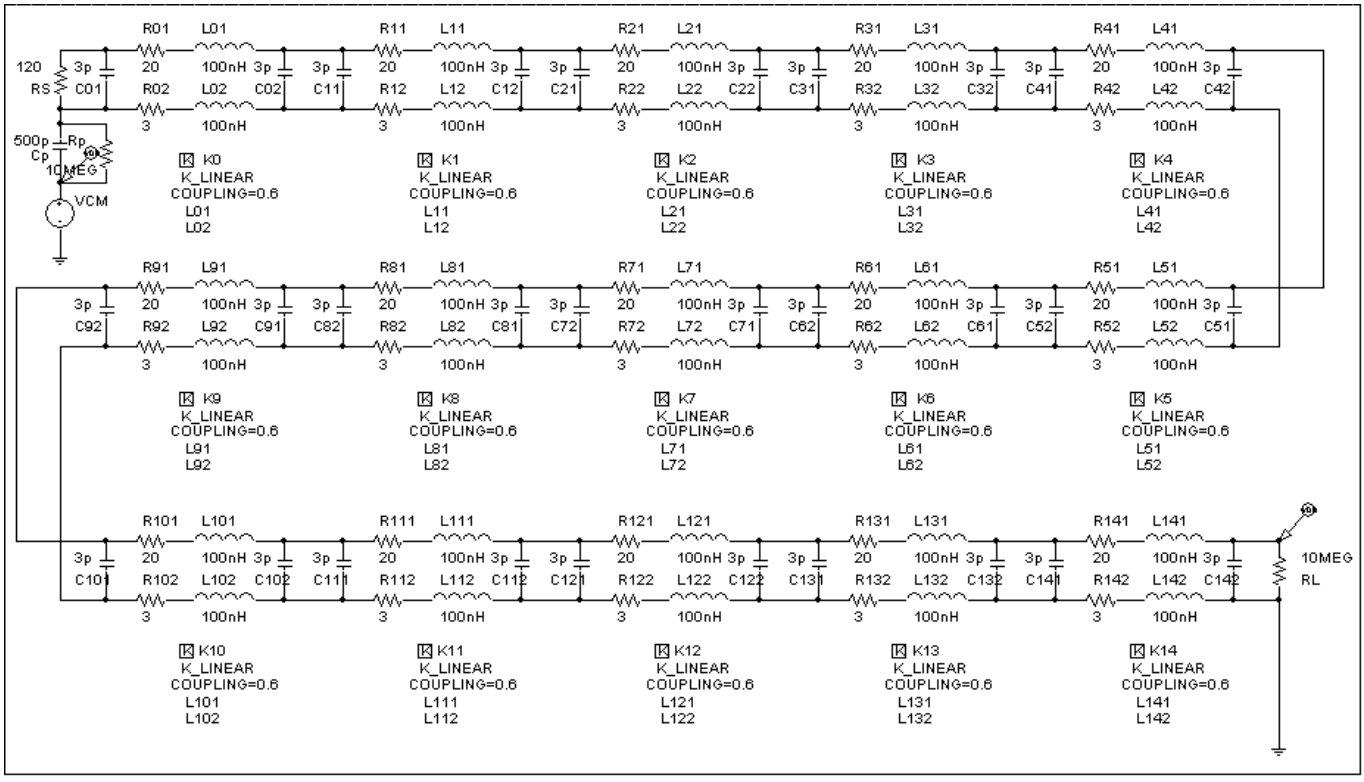

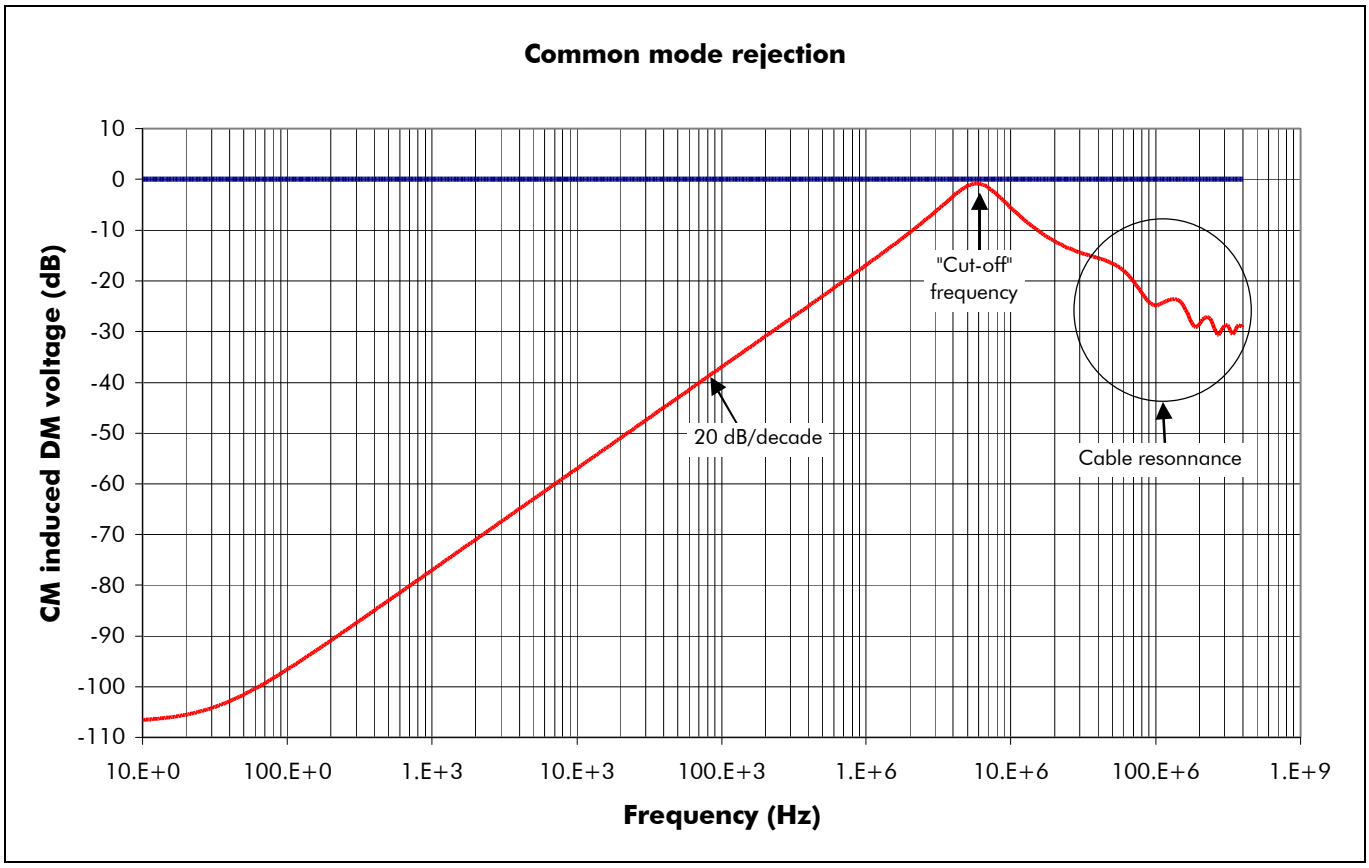

Depending on the link of interest noise specification, it may often be necessary to filter the receiving side in HF (above ~ 1 MHz), where the CMRR of the link becomes very bad, in order to limit the HF spurious to an acceptable level.

The theory developed here above is in particular applicable to the following bias links from SVM to PLM, that all have the bias return grounded on the load side (RF design) :

- HIFI FCU to FPU (mixers and amplifiers)
- HIFI LCU to LOU
- LFI DAE Control Box to FPU and to BEM trays

The same kind of frequency response is expectable from all other Instruments bias lines, even in cases where both end are isolated from chassis (one parasitic capacitance on each end is to be considered) or where the source end instead of the load end is grounded.

The HF spurious resulting from the CMRR degradation with frequency is liable to cause parasitic modulation of a RF signal : a good example is HIFI FCU to FPU IF mixers and amplifiers bias lines, cf. § 5.8.3.

HF spurious can also be converted into LF spurious because of the non-linear behaviour of electronic parts. Such phenomenon is referred to as “parasitic demodulation”, “envelope detection” or “audio-rectification” in the literature. It is tricky to simulate and is often discovered for the first time during EMC testing (RS or HF Bundle Current Injection). Such behaviour was discovered for example on MSG SEVIRI for 1 V/m @ ~ 120 MHz. High frequency EMI rejection techniques are dealt with in § 5.3.2.

5.3.1.2 Balanced analogue differential links CMRR

Most of the low frequency low level signal lines on both spacecrafts (i.e. above all the Instruments detection lines) are balanced differential.
Similarly to the unilateral connection of analogue 0V lines to chassis, the balanced differential lines have a CMRR decreasing with the frequency, because of the combined effect of :

- the board to chassis parasitic capacitance on the side where the analogue 0V is ungrounded (explained in § 5.3.1.1), allowing a spurious CM voltage source to develop a common mode current
- and of the unavoidable percentage of circuit unbalance resulting in CM to DM conversion, also decreasing with frequency due to the unbalance of parasitic capacitances

Two cases however are to be considered :

- similar impedance values on either ends of the link
- significantly different impedance values on either ends of the link

For the first case, we have the following :

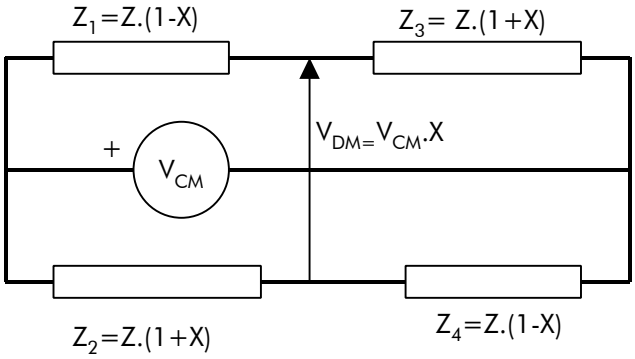

So even a very good circuit balance, e.g. better than 1%, will result in **40 dB** CMRR only (independently of the fact that the circuit unbalance may tend to increase with the frequency anyway).
That is why the unilateral grounding of analogue 0V is necessary in this case to ensure a much better low frequency CMRR for low level signal lines :

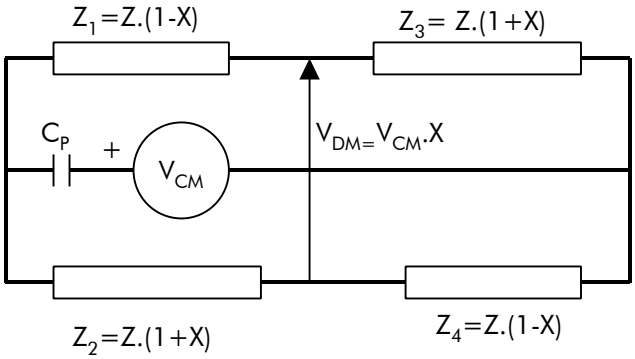

The typical corresponding CMRR variations according to frequency are shown on the following figures, borrowed from Don White (he introduces the concept of ground loop coupling, i.e. loop CM induced DM, or 1/CMRR).

GROUND-LOOP COUPLING, BALANCED SYSTEM

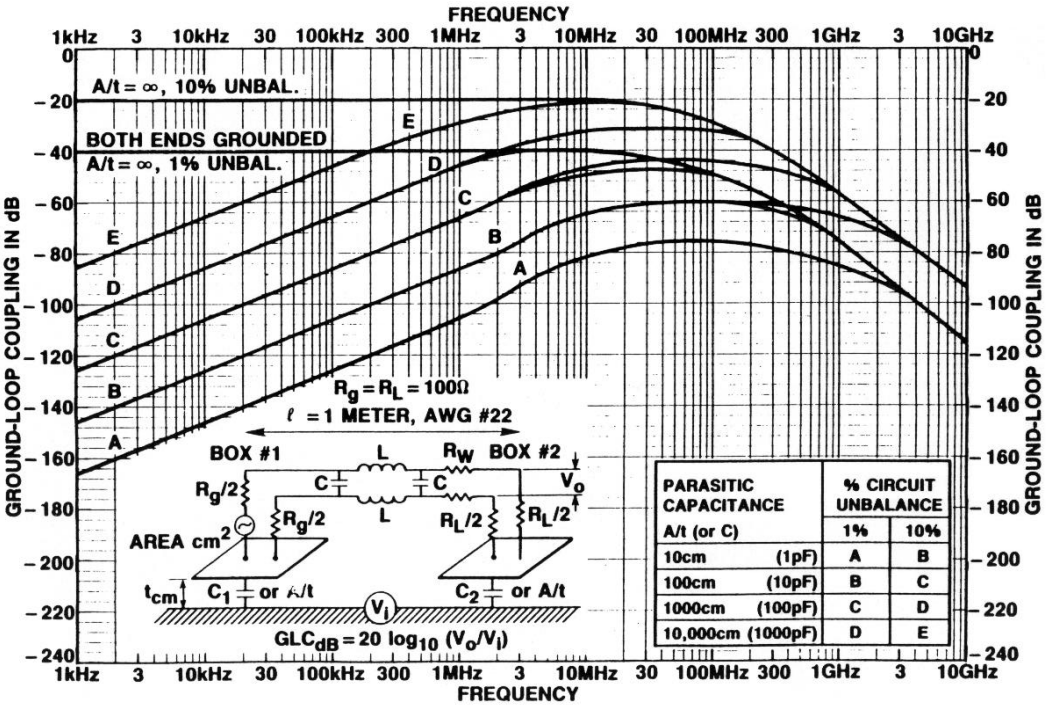

BOX -TO-BOX SEPARATION = 1 METER

GROUND-LOOP COUPLING, BALANCED CIRCUITS

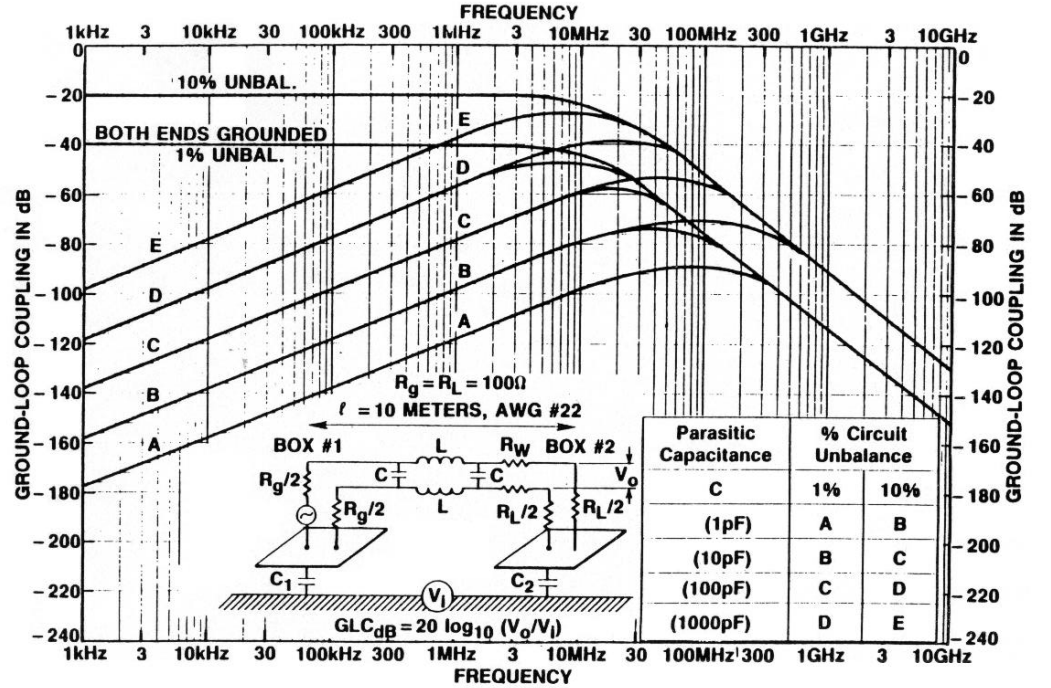

BOX-TO-BOX SEPARATION = 10 METERS

The situation is different if the impedance values on either ends of the link are significantly different :

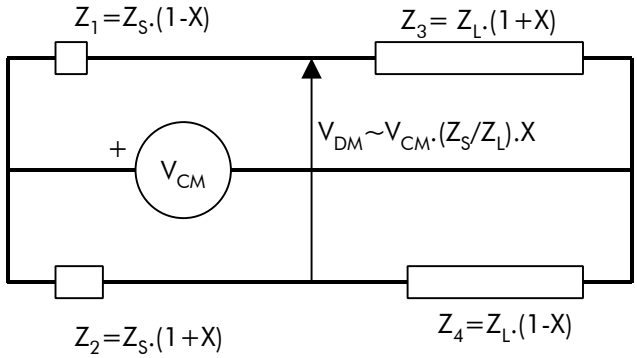

Then the CM-DM decoupling depends not only on the circuits unbalance but also on the ratio of source and load impedances.
If for example $Z_L = 1000*Z_S$ and X = 1%, we have :
$(V_{CM}/V_{DM})dB = 20\log(Z_L/Z_S) - 20.\log X =$ **100 dB**.

Such a link is then less sensitive to common mode than if similar impedance values are used on either ends.

For high impedance links, i.e. especially SPIRE, PACS and HFI bolometer – JFET links, above a certain (low) frequency, the impedances at either ends are driven by the parasitic capacitances, so taking into account the above considerations, only limited ground loop coupling rejection can be achieved above, say, 1 kHz (but for Herschel, this is the frequency above which the cryostat shielding efficiency will start to be > 40 dB, cf. § 5.4).

We have confirmed this with a rudimentary PSPICE analysis :

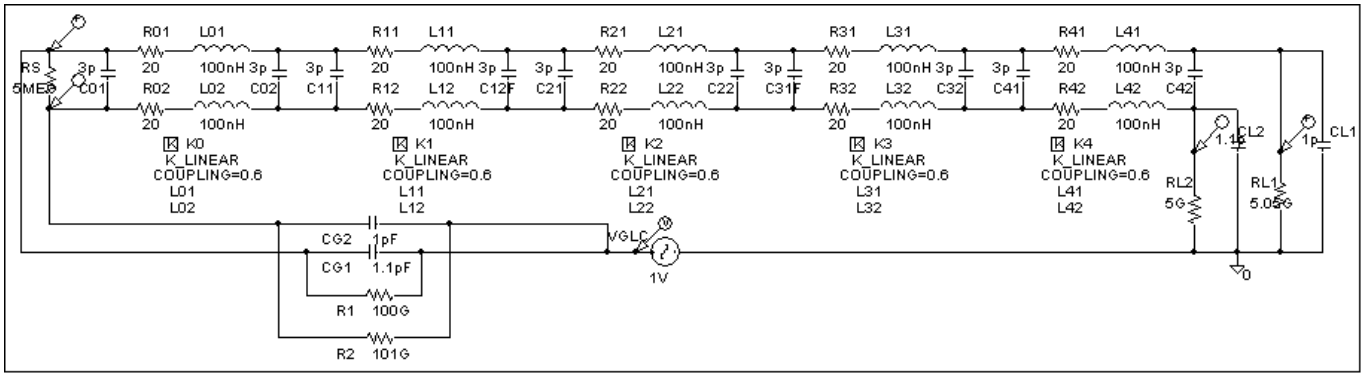

The following results show the rejection obtained from a unbalance of only 10% of the parasitic capacitances (less than 30 dB above 1 kHz) and the extra low frequency rejection obtained from the isolation from chassis :

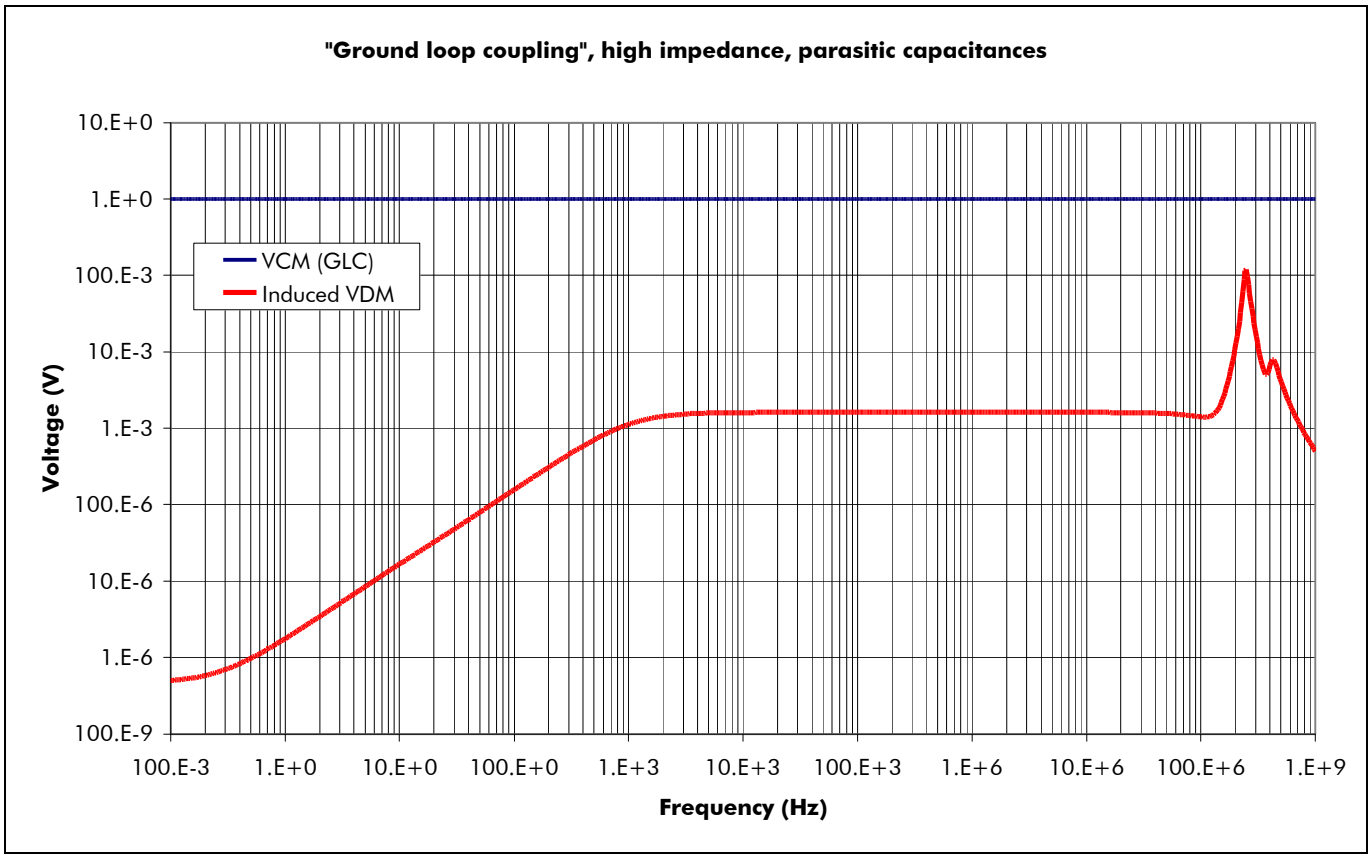

5.3.1.3 Protection of sensitive lines against low frequency EMI - synthesis

As far as the Instruments are concerned, 3 types of situations are to be considered for low frequency common mode rejection or ground-loop decoupling :

- Single ended – single ended link (e.g. the bias lines) : the bias return isolation from chassis on at least one end is neccessary and has been foreseen by all Instruments.
  The CM rejection will in any case decrease with the frequency due to the unavoidable parasitic capacitance on the isolated side(s) (cf. figure § 5.3.1.1).
  If a high frequency susceptibility of the biased circuits is expectable, a dedicated filtering is to be envisaged taking into account the specified EMC environment. That is to be assessed on a case by case basis (cf. § 5.8.3 for HIFI).
- Balanced link with similar impedance values on either ends (e.g. SPIRE FPU to SPIRE JFET and HFI FPU to HFI JFET, above 1 kHz due to the parasitic capacitances) : the CM rejection is limited by the circuits unbalance. The insulation provides additional low frequency rejection.
- Balanced link with significantly different impedance values at either ends : the situation is the same as the previous one but the impedance ratio provides additional rejection that makes the link less critical (e.g. SPIRE JFET to SPIRE DCU and HFI JFET to HFI PAU, TBC)

5.3.1.4 Shielding strategies against low frequency interference

For a shielded link, it must be noted that the connection of the shield on both ends improves a lot the CMRR above ~ 1 MHz but degrades it at low frequency. This is an exception to the overall rule of connecting shieldings at both ends : if we have a low level low frequency analogue signal (such as detectors signals or detector bias), the shield should be connected to chassis at one end only, where the return is already connected :

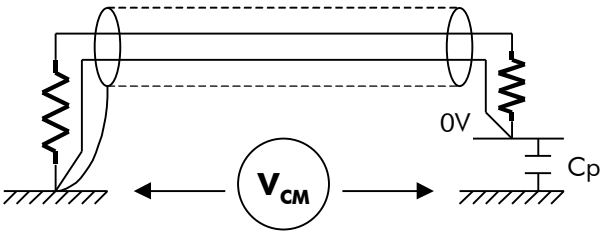

Such a shielding will protect the link against low frequency E field or low frequency capacitive crosstalk.

It will provide no protection against low frequency magnetic field or low frequency inductive crosstalk.

The worst potential threat to the detection chains is the low frequency magnetic field (cf. § 5.5) **and low frequency magnetic coupling mechanism such as inductive crosstalk (i.e. mutual inductance).**

5.3.2 Protection of sensitive lines against high frequency EMI

We have seen that the means to protect the detection chains against EMI at low frequency have virtually zero efficiency at high frequency.

So supplementary measures need to be taken to protect the detection chains against high frequency EMI as well. This can be achieved via :

- detection units or chains enclosures designed like Faraday cages
- interfaces HF or RF filtering
- cryo-harness overshielding : this point will be addressed in § 5.9 from an ESD assessment point of view but the same measures are efficient for detection chains protection against HF field to cable coupling, **cf. § 5.6**.

5.4 Cryostat shielding efficiency

The cryostat shielding efficiency was assessed in [AN-1].

The outcomes are that considering the cryostat top opening as the main shielding efficiency limitation, such mask as the following could be taken into account to convert the RS field levels specified outside the cryostat to field levels specified inside.

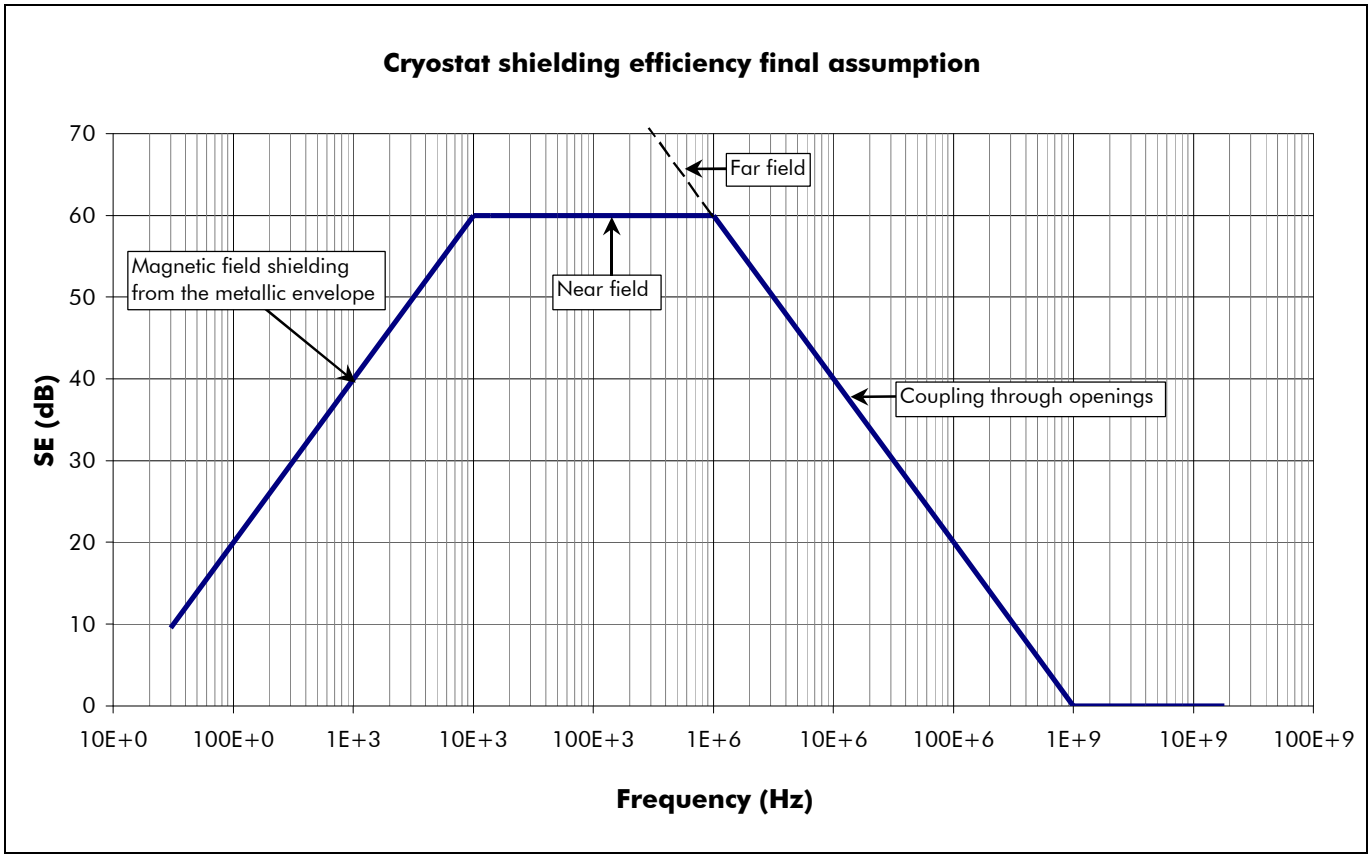

At low frequency one can distinguish magnetic and electric shielding efficiencies, the worst of the two being by far the magnetic one (actually only magnetic field RS is specified at low frequency, i.e. from 30 Hz to 50 kHz, the electric field RS starting at 14 kHz only).

At high frequency the shielding efficiency is classically driven by the openings and decreases like 1/f.

The attenuation of the specified external fields (RS E and H field specs) by the cryostat envelope leads to the field values shown on the following figure.
The Instruments are encouraged to use these values as inputs to their detection chains EMC analyses, as far as the part internal to the cryostat envelope is concerned.

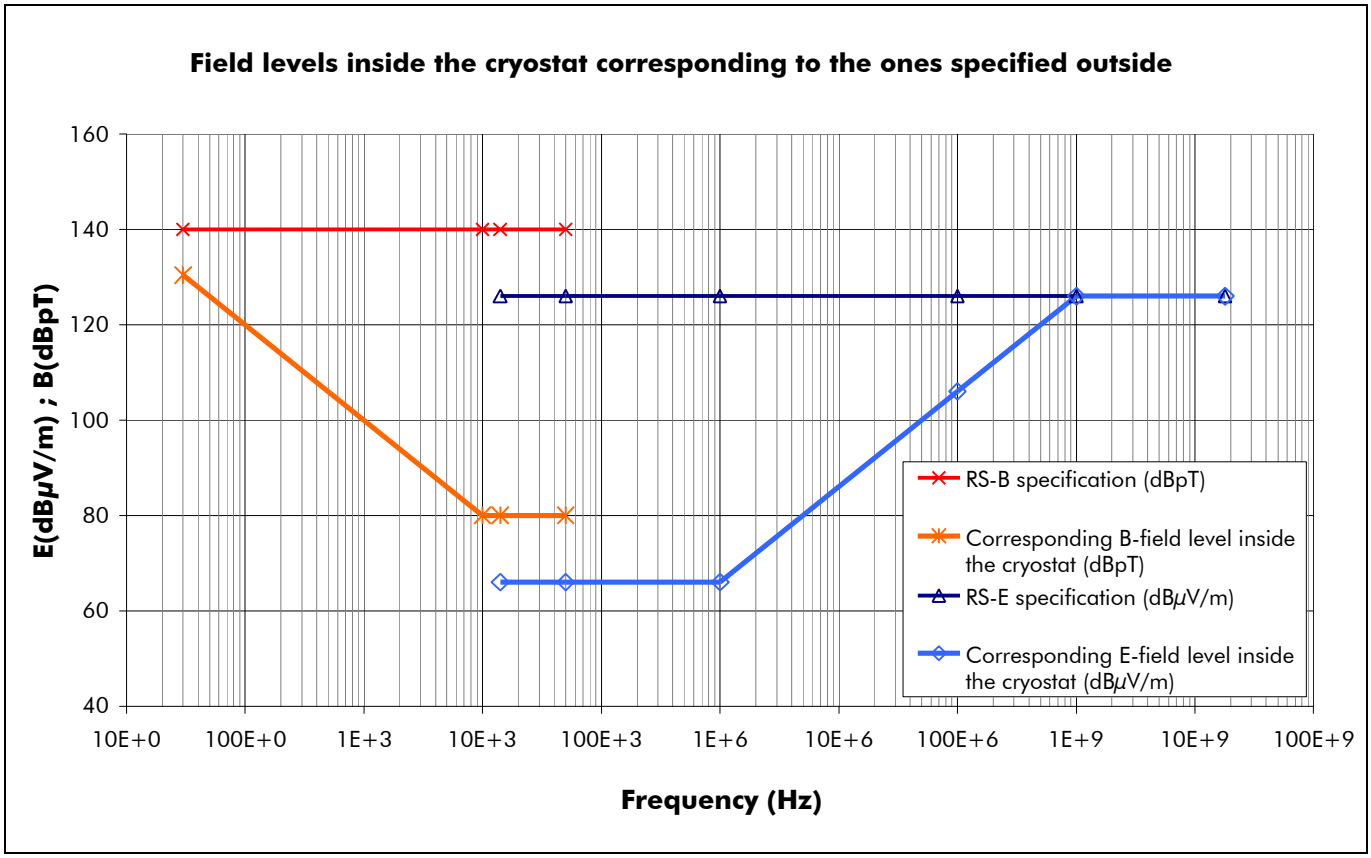

5.5 AC magnetic field coupling to detection chains

The variation of the magnetic flux inside a loop creates a open circuit common mode voltage source (§ 5.3.1 V_{CM}) that depends upon the loop surface S, the magnetic flux density B and the frequency, and can be evaluated with the simple following formula :

$V = B.S.2\pi.f$

In order to calculate the noise picked up by Herschel detection chains when submitted to an AC magnetic field, we propose to consider the following loops :

- External loops formed by the SVM structure, two adjacent external cryo-harness bundles, and the CVV structure
- Internal loops formed by one internal cryoharness bundle, the FPU and OB structures, the cryogenic piping, and the internal cryostat enveloppe

Taking into account the specified magnetic field Radiated Susceptibility level and frequency range (IID-A § 5.14.3.12 : 140 dBpT from 30 Hz to 50 kHz), we obtain the following open circuit induced CM voltage source values :

	Loop surface considered outside cryostat (m^2)	0.2	Loop surface considered inside cryostat (m^2)	0.5
Frequency (Hz)	External magnetic flux density (dBpT)	B-field induced CM voltage source on external cryo-harness (Vrms)	Internal magnetic flux density (dBpT)	B-field induced CM voltage source on internal cryo-harness (Vrms)
30	140	377.E-6	130	298.E-6
10.0E+3	140	0.13	80	314.E-6
50.0E+3	140	0.63	80	1.6E-3

For the external loops, as we are considering them as being formed by two adjacent bundles, only half of the calculated CM voltage source is applied to a given bundle, so we could divide the above values by 2.

Note 1 : these values constitute **somewhat artificial** worst cases as :

- they suppose an field uniform and orthogonal on the whole loop surface
- the 140 dBpT value is meant to be the field level at 5 cm from a unit emitting 60 dBpT at 1 m ($1/R^3$ decreasing law)

Note 2 : the actual low magnetic field sources to take into account in the [30 Hz – 50 kHz] range will be a priori the Solar Array and the Instruments FPU mechanisms.
The field levels emitted by the S/A panels minimised at the harmonics of the shunt regulators switching (frequency ~ 3 to 5 kHz) **will have to be minimised by a proper string and string polarity layout.** This is particularly important for Herschel given the position of the Solar Array.
The magnetic field emission from the Solar Array will have to be evaluated by ASED at a later stage.

The magnetic field emission from the mechanisms is to be assessed and taken into account by the Instruments in the frame of their EMC analyses. However as most of it is low frequency noise, a priori synchronised with the detection modulation frequencies, the detection chains may be intrinsically immune to that kind of noise, TBC by the Instruments.

Note 3 : the loop surface considered outside the cryostat is not meant to be accurate, just an order of magnitude based on a "best guess", allowing to derive the induced CM voltage sources order of magnitude.
From the considerations of § 5.3.1 it appears that the low frequency common mode rejection provided by the unilateral analogue 0V grounding should be ~ 40 dB at 50 kHz and the balance of detection links another 40 dB. If we can demonstrate at a later stage that the magnetic field RS specification at 50 kHz is oversized by, say, 60 dB as far as the actual magnetic field imposed to the external cryo-harness is concerned, we end up with a spurious induced voltage lower than **0.1 µV**, without even considering any additional filtering.

The frequency considered (50 kHz) being significantly out of the detection bandwidths, that order of magnitude of EMI can be expected to be acceptable, **TBC**.

Note 4 : should the test results on Herschel PLM EQM show an Instrument susceptibility to AC magnetic field threatening the System margin, one option allowing to reduce the loop surfaces would be to connect the bundles overshieldings to the lower part of the CVV :

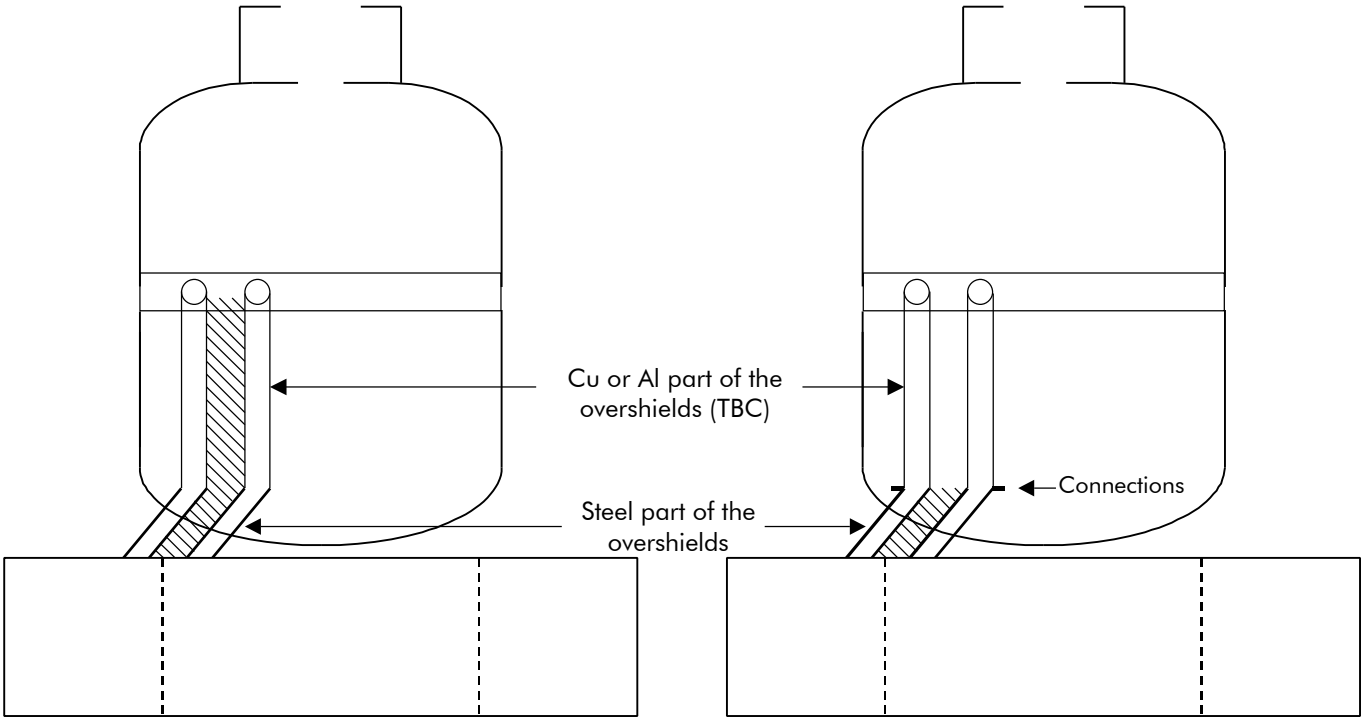

Loop surface reduction option

Unlike a direct CVV – SVM connection, this option would not introduce any additional thermal leakage. Moreover it must be noted that even if direct connections (like aluminum tape straps along the GF struts) would exist between the CVV and SVM structures (NOT intended), it would not reduce the surface of the biggest loops that would still be the ones between two adjacent bundles.
These loops only are relevant, not the ones between a given bundle and some imaginary spacecraft continuous group plane that obviously does not and cannot exist.

5.6 E-field coupling to detection chains

The noisy electronics, such as DC/DC switching converters, digital signals and clocks, and the RF units are sources of E-field emission on board. In order to guarantee a functioning margin with respect to the sensitive electronics susceptibility, a RS E-field specification is applicable to the Instruments that is 2 V/m from 14 kHz to 18 GHz (IID-A § 5.14.3.10).

Simple formulas exist allowing to compute the common mode voltage induced in a loop submitted to an incident E-field, considering the following worst case assumptions :

- loop submitted to an homogenous field in far field conditions
- electric field parallel to one of the sides of the loop i.e. magnetic field othogonal to the loop plane
- propagation vector in the loop plane

Then two cases are to be considered :

- cable length $< \lambda/4$ i.e. length(m) < 75 / F(MHz) :
$$V(V) = \frac{l(m) \times h(m) \times F(MHz)}{48} \times E(V/m)$$
- cable length $> \lambda/2$ i.e. length(m) > 150 / F(MHz) : the induced voltage **goes through maxima and minima** according to the ratio between l and $\lambda/2$, but the maxima are not higher than : V(V) = 2.h.E(V/m), independant from F

If we consider again the (somewhat arbitrary for now) 0.2 m^2 loop surface of § 5.5 and a loop length of 3 meters, the induced loop voltage corresponding to the IID-A RS-E requirement would be the following :

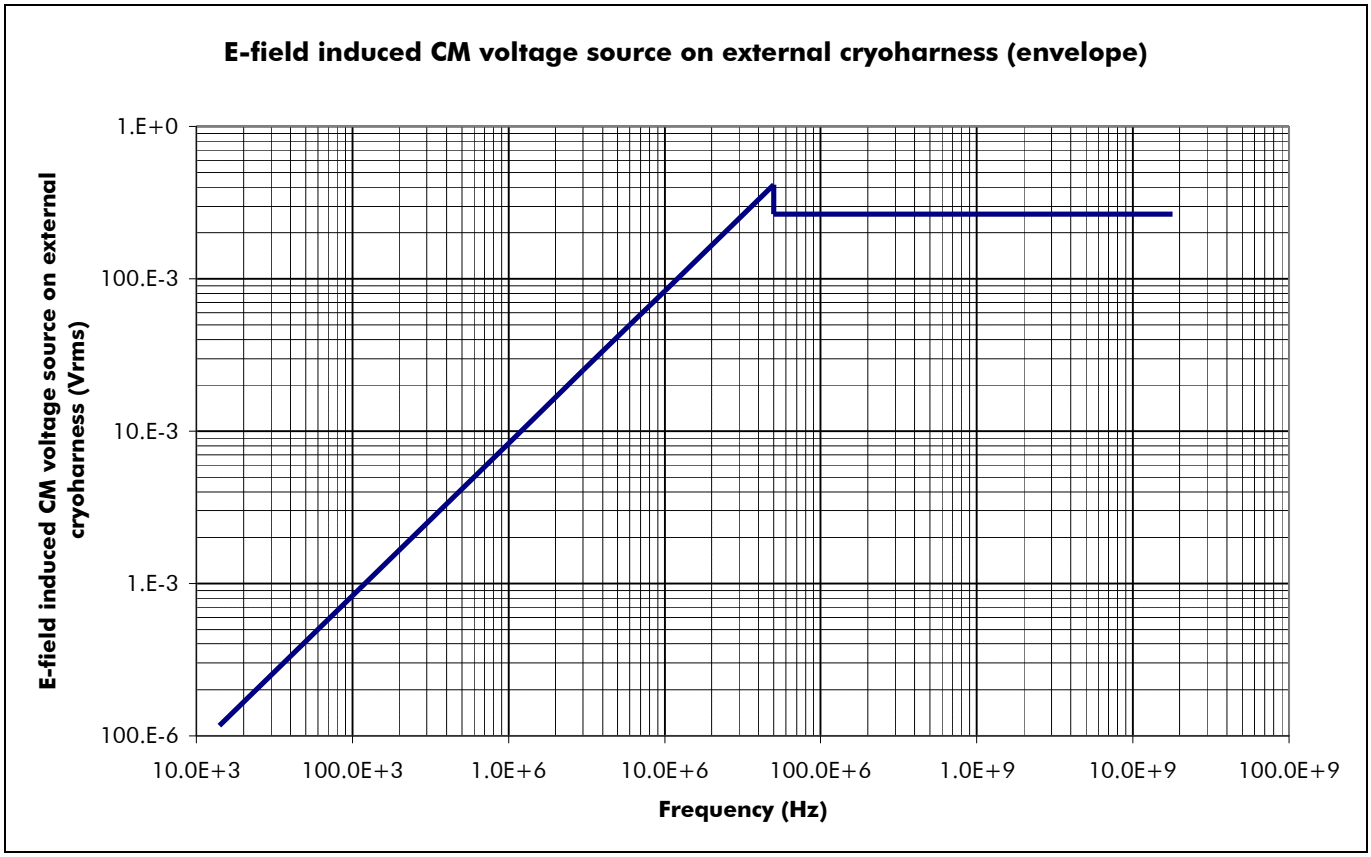

At the frequencies where the developed CM voltage is significant, a technically correct evaluation of the coupling to the internal links should involve the overshielding transfer impedance concept, recalled in § 5.9.1 of the present note.

The differential voltage induced on a balanced link (such as most detection chains) through the transfer impedance can then be computed as follows :

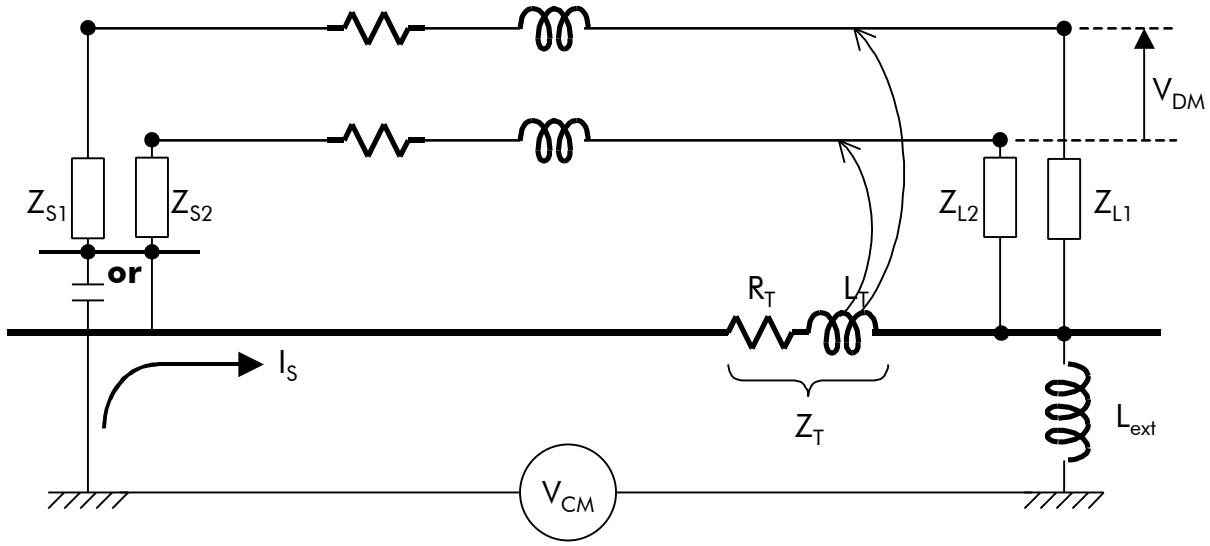

$Z_{S1} = (Z_S/2).(1 \pm X)$ $\qquad$ $Z_{L1} = (Z_L/2).(1 \pm X)$

$Z_{S2} = (Z_S/2).(1 \pm X)$ $\qquad$ $Z_{L2} = (Z_L/2).(1 \pm X)$

$$V_{DM} = \left(Z_T \times \ell \times I_S\right) \times X \times \frac{\min\left(Z_S, Z_L\right)}{Z_S + Z_L} \text{ with } I_S = \frac{V_{CM}}{Z_{loop}}$$

$$\Rightarrow \boxed{V_{DM(internal)} = V_{CM(external)} \times \frac{Z_T \times \ell}{Z_{loop(external)}} \times X \times \frac{\min\left(Z_S, Z_L\right)}{Z_S + Z_L}}$$

The term $Z_T \times X \times \frac{\min\left(Z_S, Z_L\right)}{Z_S + Z_L}$ is sometimes mentioned in the literature as "differential transfer impedance", Z_{TD}.

However, we think it is easier to follow the next steps :

- Calculation of external common mode voltage source V_{CM}(external), from the external loop characteristics and from the external field value ;
- Calculation of the induced internal common mode voltage source, taking into account the overshielding transfer impedance Z_T and the external loop impedance :

  $$V_{CM(internal)} = V_{CM(external)} \times \frac{Z_T \times \ell}{Z_{loop(external)}} \text{ ;}$$

- Calculation of the CM-induced DM on the internal signals, taking into account the percentage of unbalance, the impedance ratios, and the eventual analogue 0V isolation from ground on one end.

At frequencies where the cable is electrically short, Z_{loop} should be taken as the self inductance of the loop considered with a classical value of order of magnitude 1 μH/m.
At frequencies where the cable is electrically long (length $\lambda/4$ at 25 MHz in our example), Z_{loop} should be taken as the characteristic impedance of the external line, formed by the overshielding of the cryo-harness bundle of interest and the one of the next bundle (cf. figure § 5.5), with a typical order of magnitude of, say, 400 Ω.

[this value was calculated considering the line formed by 2 overshielded bundles, considered from the outside, an applying the literature formulas for a 2-wires line far from a ground plane :

$$C \approx \frac{\pi\varepsilon_0}{\mathrm{Ln}\frac{D}{a}}\ \text{(F/m)},\ L \approx \frac{\mu_0}{\pi}\cdot\left[\mathrm{Ln}\frac{D}{a}+\frac{\alpha}{4}\right]\ \text{(H/m) with } \alpha=1 \text{ at LF / } \alpha=0 \text{ at HF, and } Z_C \approx \sqrt{\frac{\mu_0}{\varepsilon_0}}\cdot\frac{\mathrm{Ln}\frac{D}{a}}{\pi}$$ **]**

Similarly, the total transfer impedance to take into account should be $Z_T(\Omega/m)$ x length when the cable is electrically short and $Z_T(\Omega/m)$ x $\lambda/2$ when the cable is electrically long.

With as reasonably as possible assumptions on the various parameters at this stage, recalled in the following table :

Loop surface (m^2)	0.2		
Loop length (m)	3	External indutance (H)	2.1E-6
Height (m)	0.067	External Zc (Ohms)	400
Corner frequency (Hz)	50.E+6	Assumed transfer resistance (Ohms/m)	100.0E-3
E-field level (V/m)	2	Assumed transfer inductance (Ohms/m)	3.3E-9

… we obtain the following results for V_{CM}(external), Z_{loop}, I_S, Z_T and V_{CM}(internal).

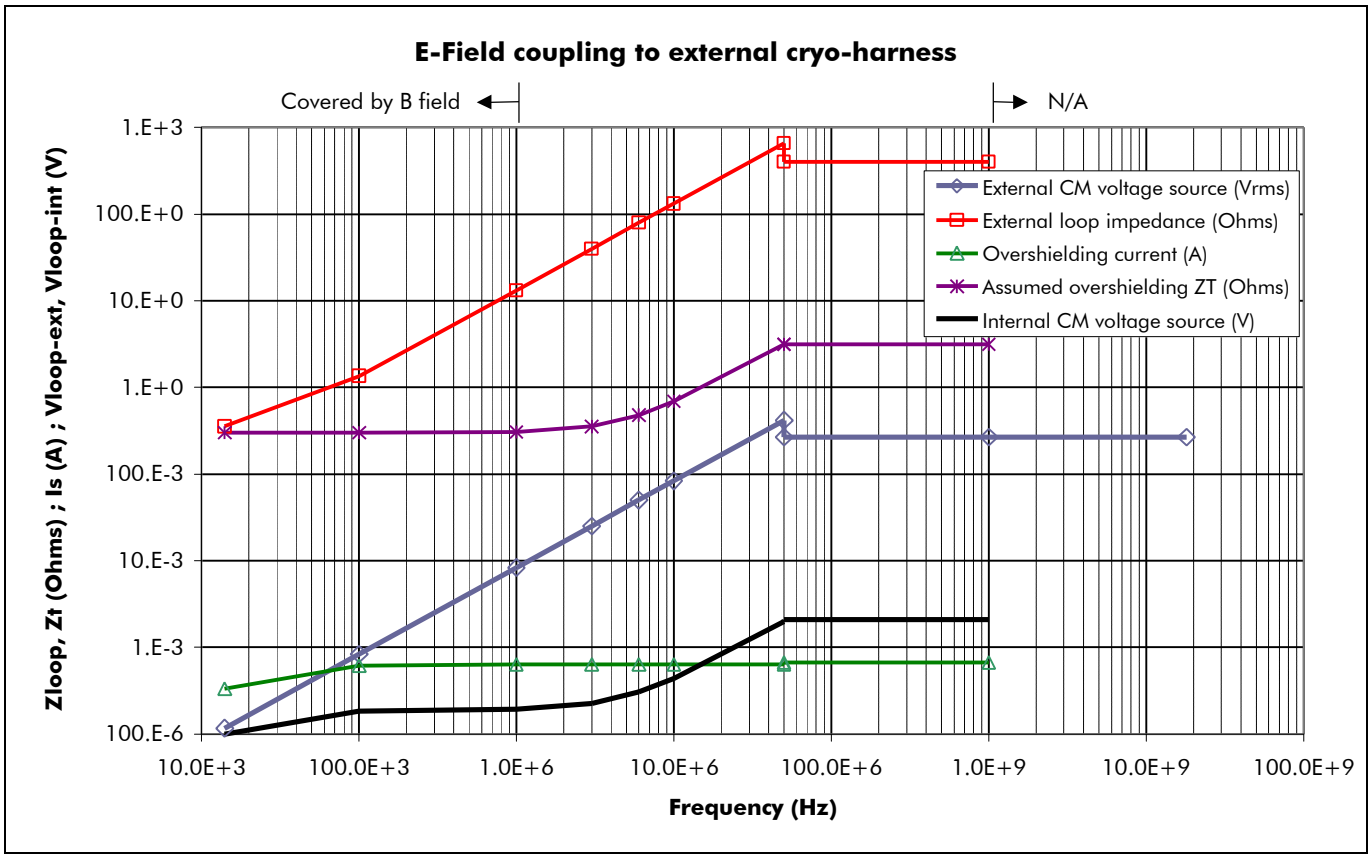

Again, the above is meant to suggest methods that can be used to derive spurious signal levels from the specified RS specifications, and to propose orders of magnitude. It is not supposed to replace the network simulations that are on going under the Instruments responsibility.

The method is certainly not suitable above 1 GHz and under 100 kHz the E-field coupling is covered by the magnetic field coupling, expected to be significantly more severe, cf. § 5.5., so the remaining relevant band for E field to cable coupling on the external cryo-harness is between 100 kHz and 1 GHz.

The induced spurious DM voltage on the various sensitive signals can be derived from the above "internal CM voltage source" taking into account the performance of the Common Mode rejection methods recalled in § 5.3.1 and the eventual implemented filtering.

They are then to be compared to the Instruments out-of-band interference requirements on a case by case basis.

5.7 DC magnetic compatibility

According to HIFI EMC Control Plan, SRON-U/HIFI/PL/2000-002, Issue 2.0, the mixers in HIFI FPU are susceptible to static and dynamic magnetic fields and their susceptibility threshold to low frequency magnetic fields is estimated 0.25 mT (TBC), that is 168 dBpT.

If this is confirmed, no compatibility problem with the SVM units magnetic field emission is to be expected.

5.8 ASPI understanding and assessment of Instruments grounding/EMC concepts

5.8.1 SPIRE

The main grounding/EMC features of SPIRE bolometer detection chains are recalled hereafter.

5.8.1.1 Broadband interference sensitivity

From "SPIRE design description" document, (SPIRE-RAL-PRJ-000620 , issue 1.0, 04/02/2002), "bolometric detectors are sensitive to any form of power input to the device. Unwanted electromagnetic radiation (from any part of the spectrum) absorbed by the detector will generate a spurious signal. Over and above this, any spurious RF power reaching the detector through conduction along the bias or signal wires will be dissipated through ohmic heating of the thermometer element, generating a spurious signal. It is critical therefore that bolometers be protected from EMI via an effective RF shield".

Therefore the 4-K FPU and JFET enclosures will be designed to form Faraday cages.

"All sub-system wiring entering the instrument box must pass through passive RF filters mounted in boxes from the SPIRE Optical Bench on the spectrometer side. When the cover is integrated with the optical bench the RF filter boxes will be sealed to the cover."

"The exception to this are the harnesses for the detectors themselves that connect the bolometer arrays to the externally mounted JFET units. These are filtered within the JFET units and then pass to the instrument box via a drilled plate hard mounted to the SPIRE Optical Bench. The wiring harnesses therefore form part of the RF shield."

"The harness connecting the bolometer elements to the JFET units represents the most vulnerable part of the detection system." Therefore and as well "to minimise the signal loss or phase distortion due to harness capacitance, the length of the harnesses between the JFETS and the bolometers needs to be minimised. Hence, the two groups of JFETs are located on the Herschel optical bench as close to the FPU structure as is practical."

5.8.1.2 Analogue 0V grounding

The main grounding features of SPIRE bolometer detection chains are recalled hereafter :

- The two halves of the instrument, the photometer and spectrometer, are treated as entirely separate electrical systems with their own power supplies and grounding (analogue 0V sections grounded separately)
- SPIRE require that all CU's chassis are isolated from the HOB (Herschel Optical Bench)
- The loop areas in the cryoharness between detection bias lines and detection signal lines will be limited as far as possible

RAL has been performing a trade-off concerning the point of grounding of the (two) analogue 0V sections, that is either at DCU level or at detector level.

It must be noted that, especially on the high impedance part of the detection chains (between detectors and JFET), the parasitic capacitance's and their unavoidable unbalance may have a significant impact on the "ground loop" noise rejection, and not only at high frequency :

- 1 pF equals 5 MΩ at ~ 30 kHz
- 10 pF equal 5 MΩ at ~ 3 kHz
- 100 pF equal 5 MΩ at ~ 300 Hz

5.8.1.3 Synthesis

It must be noted, as explained in § 5.3, that all what can be done by playing on the analogue 0V grounding will have in any case an efficiency decreasing with frequency due to the parasitic unbalance and parasitic capacitance's, i.e. will be efficient at "low" frequency only.

Above a "certain" frequency, depending on the impedance's involved on the various parts of the detection chain, only shielding and filtering are efficient to reject the EMI.

The design is relying on the external cryoharness overshieldings, the CVV (cf. § 5.4) and the 4-K FPU enclosure shielding and RF filtering to provide the necessary high frequency EMI rejection.

5.8.2 PACS

5.8.2.1 Braodband Interference sensitivity

Like SPIRE, PACS incorporates bolometer detectors that are sensitive to many energy manifestations including RF.

The "PACS Instrument Design Description Document", PACS-ME-GR-002, part II, 28/01/2002, mentions : "The detectors we manufactured and tested in 99 [...] were easily perturbed by Radio Frequencies. Most perturbations generally affect the whole array, and show two effects at the signal level : a synchronous signal perturbation seen on all the pixels, and a higher noise level due to the temperature increase in the sensitive part of the detector."

"[Bolometer] Sub arrays are mounted in an optical-mechanical structure shielding detectors from outside possible perturbed conditions : [...] RF electromagnetic perturbations."

RF filter boxes are implemented on the Bolometer Focal Plane enclosure (4K) :

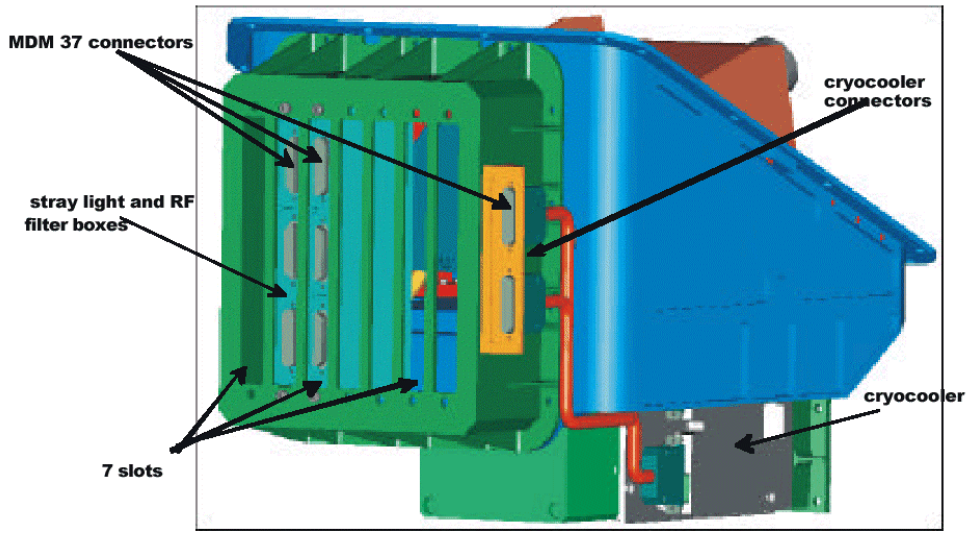

5.8.2.2 Analogue 0V grounding / filtering

Filter/decoupling capacitors will be implemented on the distribution boards inside the Ge-detector FPU, meant to reduce crosstalk and EMI.

5.8.3 HIFI

HIFI is following the usual rules of grounding applicable to RF units. In particular the bias lines supplied by warm units installed in the SVM to cold RF units belonging to the PLM (i.e. IF multipliers and amplifiers in the FPU and frequency multipliers in the LOU) have their return grounded on the RF unit side, i.e. on the cold side.

The common mode rejection of IF amplifiers bias lines is analysed in "Filtering of FCU – IF amplifiers interface" SRON-U/FCU/TN/2000-003, Draft2.

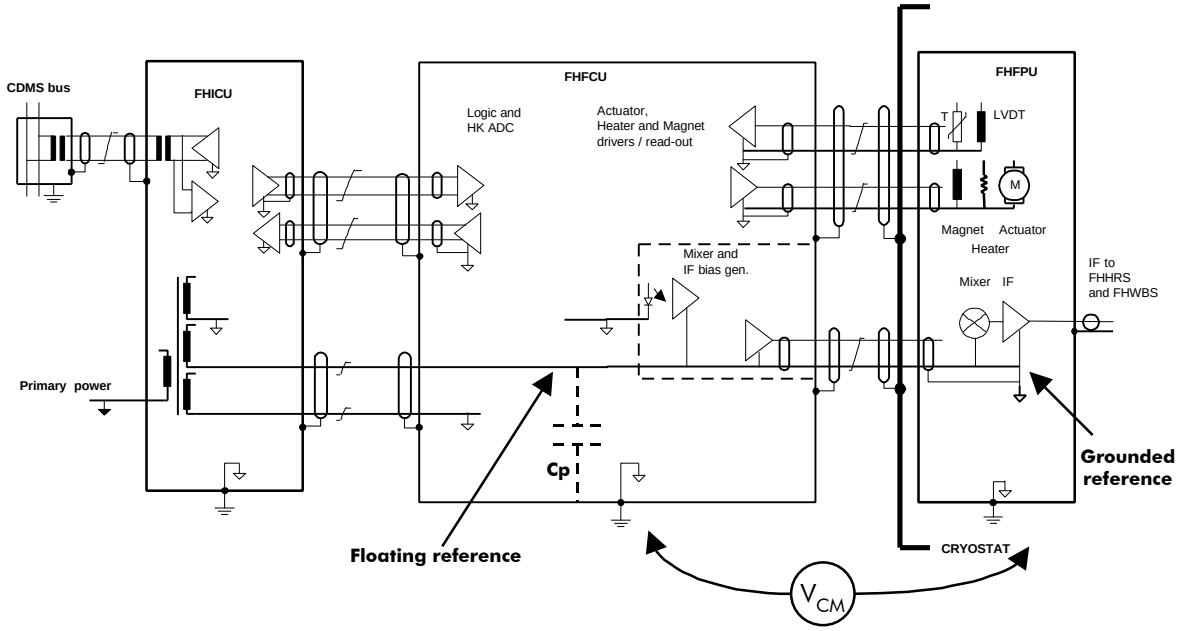

The problem is the following : the FCU delivers biases to the FPU IF amplifiers located in the cryostat at the end of 5 m cable length. The noise level on these links need to be low enough to ensure a sufficient stability of gain of the IF amplifiers.
In the FCU, the IF amplifier bias circuits are isolated from the structure in order to ensure common mode rejection at low frequency (cf. § 5.3.1.1 of the present note). However, a parasitic capacitance of several nF (probably rather conservative) is expected by SRON between these circuits and the chassis.
This capacitance, together with the resistance of the cryo return wires (estimated resistance per polarisation ≤ 50 Ω) creates a (first order) high pass filter with a w.c. cut-off frequency of 300 kHz (probably one decade lower than reality due to the conservative parasitic capacitance value assumed, cf. § 5.3.1.1) that decreases common mode rejection according to F.

SRON conclusion is that some filtering in the FPU will be necessary, i.e. for each of the 70 IF transistors :

- a drain filter consisting of a single 100 nF capacitor
- a second order low pass gate filter with 5 kHz cut-off frequency consisting of 2 resistors and 2 capacitors

The same kind of analysis was done by SRON for the mixers bias interfaces in "FCU EMC overview / mixers bias interface", FPSS-00087.

The same philosophy applies to the LCU to LOU bias lines ; the loop surface between the bias lines cryo-harness and the 14 WG casually ensuring the chassis connection between the SVM (through the LSU unit) and the LOU should be reduced to the minimum possible (close routing) to reduce low frequency magnetic field susceptibility.

5.8.4 LFI

Like HIFI, LFI is following the usual rules of grounding applicable to RF units.
In particular the bias lines supplied by the DAE Control Box installed in or on the SVM to the RF units belonging to the PLM (i.e. FEM and BEM) have their return grounded on the RF unit side (FPU side for the FEM bias and phase switch bias, and BEM side for the BEM and analogue acquisition bias).

The FPU 20 K enclosure forms a Faraday cage, the weakest point of which is the cryo-harness providing bias from the BEU (precisely the DAE lateral trays) to the FPU.
It is a flat cable featuring a film shielding on both sides (100 nm thick vapour deposed aluminium), connected to chassis at both BEU and FPU sides.

It may also be particularly sensitive to low frequency magnetic field (cf. § 5.5) and so the loop surface between the cryo-harness and the WG's should be reduced to the minimum to limit the magnetic field to loop coupling.
However a priori the potentially significant LF AC magnetic field sources (the solar array and the 4K cooler) are not close to this loop, and one can rely to some extent on the benefit of the $1/R^3$ decrease law.

Zener diodes are used in the BEM to protect the MMICs from possible over-voltage peaks externally induced by EMI (§ 6.6.2.3.1 of LFI design report, PL-LFI-PST-RP-002).

5.8.5 HFI

5.8.5.1 Braodband Interference sensitivity

The 4K stage, the JFET box, and the SST bellow in between provide an electromagnetic shielding (a Faraday cage) for the high impedance part of the Readout Electronics, i.e. the part most sensitive to E-field and capacitive coupling (idem SPIRE).

The JFET → PAU harness is also protected inside a bellow, against field to cable coupling and ESD.

5.8.5.2 Bonding / Analogue 0V grounding

The PPLM bonding aims at avoiding DC loops involving HFI cryo-harness bellows, at least between the 4K enclosure and the JFET box, the idea being to cancel AC magnetic field to loop coupling.

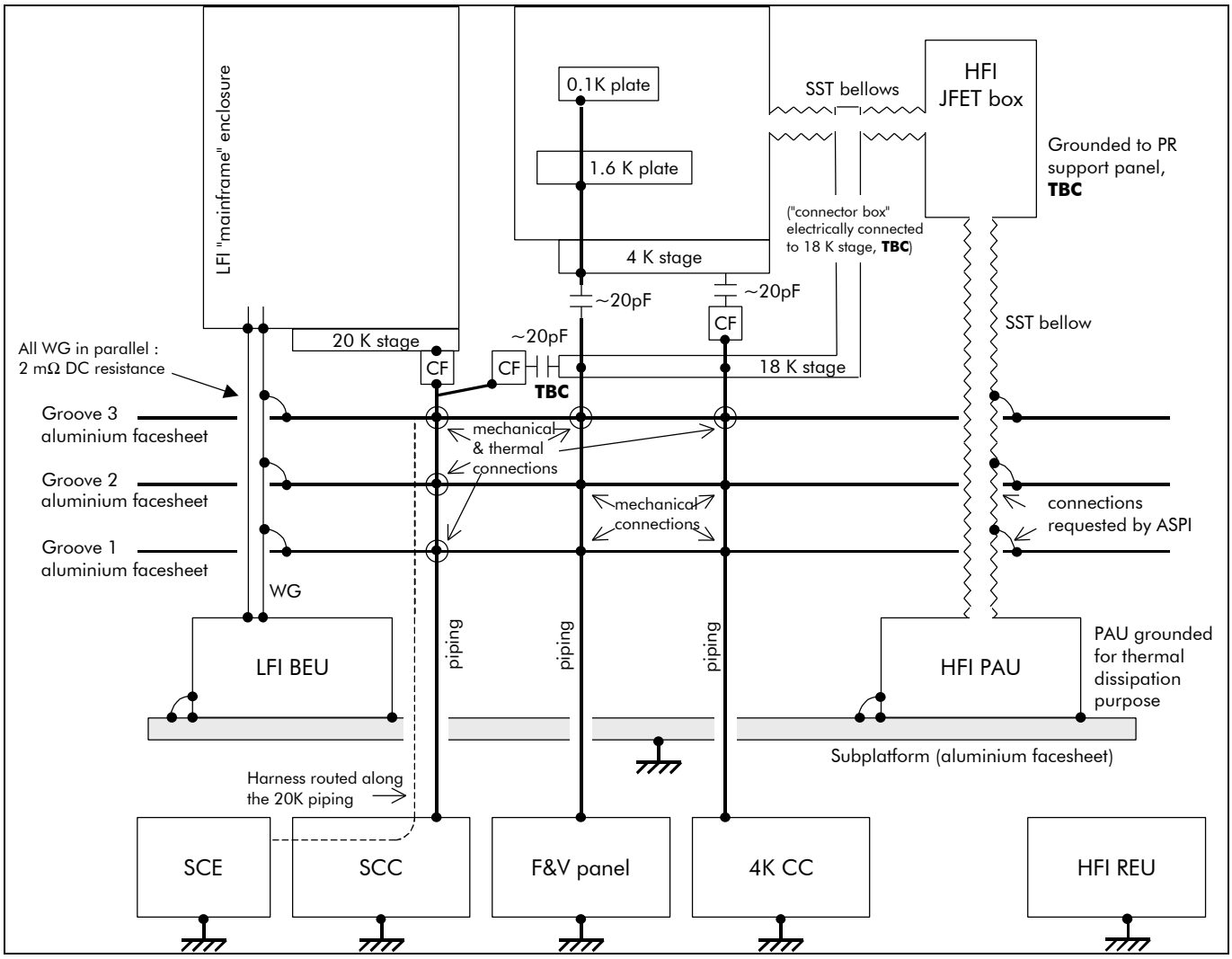

On the contrary, within the volume between groove 3 and the subplatform, a lot of DC loops involving the bellow between the JFET box and the PAU exist.

The GLC resulting in DM signal will depend on :

- The “mechanical dissymetries”
- The JFET CMRR, which cannot be higher than 60 dB

Concerning the AC loops or AC coupling with LFI, HFI EMC team are concerned about the high parasitic capacitance at the mechanical interface between FPUs, estimated ~ 200 pF, liable to transmit “medium” frequency noise (i.e. 10 to 100 kHz).

5.9 Protection of external cryo-harness against ESD

SRS SENV-155 requires that :
" […] The spacecraft shall withstand without being disturbed, the following levels:
- For Conducted Electrostatic Discharge (current injected anywhere in the structure) :
  - Energy: 15 mJ
  - Voltage: 15 kV (may be reduced to 4 kV if risk for is apparent)
- For Radiated Electrostatic Discharge (spark gap at 30 cm distance)
  - Energy: 15 mJ
  - Voltage: 15 kV "

That is to say that independently from the analyses carried out in parallel to assess the spacecraft's charging during transfer orbit and cruise to L2, the spacecraft's are required to be designed so as to be able to survive a typical flight ESD.

It must be noted that the a.m. requirement is not complete as the current rise time and peak value, that drive the transient spectral content, and thus coupling, to cables and circuits, are not specified.
However the typical values are known and we will take them into account : current rise time t_r = 5 to 10 ns, current peak value 50 A_p worst case. The corresponding frequency $1/\pi t_r$ would then be 30 to 60 MHz that is to say high frequency with respect to cables behaviour.

Because of the detection chains low frequency rejection constraints mentioned before, most of the Instruments cold harness shielding will be connected to chassis on one end only (either SVM or FPU end). As explained before, this does not bring any high frequency rejection.

On Herschel especially, the external cryo-harness that is exposed to space needs to be protected against the occurrence of an ESD current flowing, e.g. between SVM and PLM (the requirement mentions a "current injected anywhere in the structure").

Both theory and experience allow to predict that hundreds of volts can be reached at interfaces in case a system involving unshielded cables (or cables with poor quality shielding connections to ending units chassis) is subjected to an ESD. Such an experiment is described in Michel Mardiguian's "Electrostatic Discharge, Understand, Simulate and Fix ESD Problems" book, ISBN 0-932263-27-5, chapter "ESD Protection of External Cables".
It doesn't matter then whether this voltage is common mode, differential mode, or whether the interface is single ended or differential. As explained before, an unshielded or badly shielded link involves a rejection ratio close to 0 dB at the frequencies of interest.

The conclusion of the a.m. external cables chapter is reproduced hereafter (if it can help to convince anybody still being sceptical) :

> "To reduce ESD pick-up, a cable shield must be bonded to each housing that it penetrates.
> The argument that a floated shield will not allow the ESD current to flow and, therefore, will avoid coupling does not stand a more thorough analysis : the floated end of the shield would reach several hundred volts of common mode voltage and would re-inject some of it by capacitive coupling (more precisely transfer admittance) on the wiring."

That is why, taking into account both Instruments requirements to have their external cryo-harness overshielded (IID-B's 2.0, also cf. [GND-1]) and ESA requirement that spacecraft's should be able to " withstand without being disturbed" a typical ESD, **it has been chosen by ASPI to consider as a baseline that Herschel external cryo-harness will be overshielded, with continuity over 360° with warm units chassis on one end and CVV enclosure on the other end**.

In order to assess the impact of an ESD on such a shielded bundle, it is necessary to be able to model the coupling between a structure current flowing on the overshielding and the cables inside.

5.9.1 Recalls on transfer impedance theory (Zt)

The best theoretical tool to assess for a harness shielding or overshielding performance is the transfer impedance. This theory is recalled hereafter :

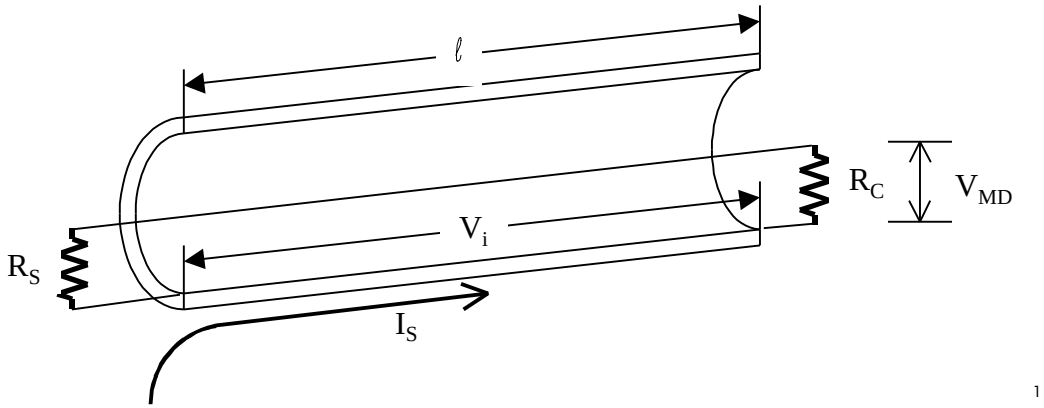

[1]

$l < \lambda/2$

In a shielded cable, the current induced on the shield by an external perturbation creates inside a longitudinal induced voltage V_i that distributes itself between the charging loads.

The transfer impedance is defined as $Z_t = \frac{V_i}{I_S \times l} = \frac{2V_{MD}}{I_S \times l}$ if $R_C = R_S$

Z_t is expressed in Ω/m and characterises the shielding imperfection.
The better the shielding is, the lower Z_t is.

At low frequency (up to 10 or 100 kHz) Z_t is constant and equal to the shielding resistance.

For cables having a tubular shield (e.g. coaxial semi-rigid cables) Z_t is only driven by the diffusion of the electromagnetic fields through the tube (i.e. skin effect), and expresses as follows :

- At low frequency ($T/\delta < 1$) :

$|Z_t| = \frac{1}{2\pi a \sigma T} = R_0$ with :

a : shield diameter
σ : shield conductivity
T : shield thickness

δ : skin depth : $\delta = \frac{1}{\sqrt{\pi \mu \sigma f}}$

R_0 : DC resistance of the shield per unit length

[1] From Mardiguian « Manuel pratique de compatibilité électromagnétique »

- At high frequency (T/δ >1)

$$|Z_t| = 2\sqrt{2} \cdot e^{-T/\delta} \cdot R_{hf} \text{ with } R_{hf} = \frac{1}{2\pi a \sigma \delta}$$

Braided-wire shields have a different behaviour at high frequency, especially because of the coupling by diffraction through the holes.
For most simple-braided shields, the transfer impedance can be expressed as :
$Z_t = R_0 + jL_t\omega$
(R_0 being the diffusion component, and L_t the transfer inductance expressing the magnetic field penetration through the holes).

Some more complex coupling phenomena exist for braided shields that depend on the geometry : number of carriers (bands of wires) that make up the shield, number of carrier crossings per unit length, weave angle…

In the end, the following typical Z_t curves can be met :

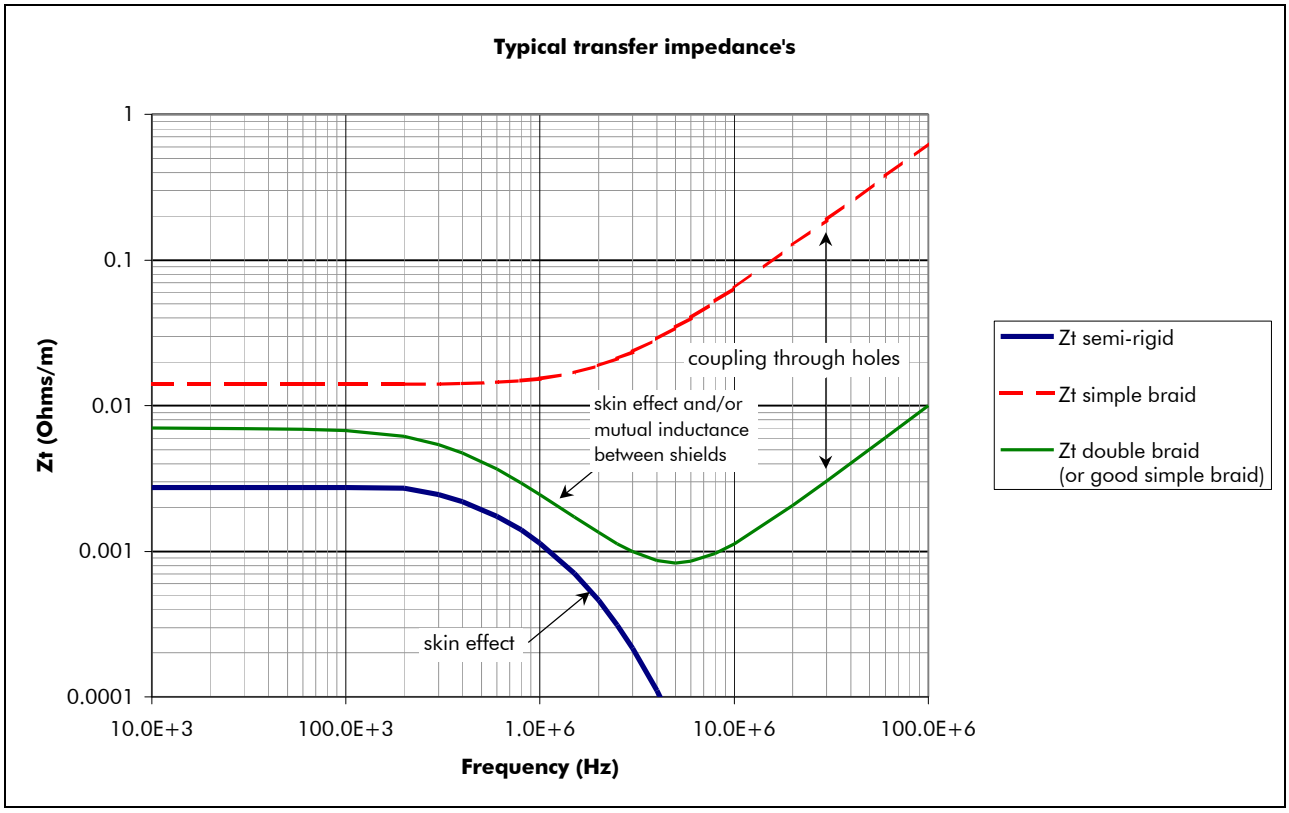

Considering that thermally insulated cables will be used, the low frequency plateau will be higher of a couple orders of magnitude, but the general behaviour will remain the same, in other words :

- HIFI IF semi-rigid cables should have a low Z_t at the frequencies corresponding to the ESD spectral content and thus the IF interfaces at FPU and Warm Units sides respectively should be well protected ; that is to be confirmed by the cables characterisation.
- The external cryo-harness bundles overshielding Z_t is expected to be on the +20 dB/dec part of the curve at the frequencies corresponding to the ESD spectral content, i.e. the optical coverage driving the diffusion component should drive the Z_t at the frequencies of interest.

5.9.2 ESD coupling mechanisms to circuits

The coupling mechanism of an ESD flowing on the external cryo-harness overshieldings to the Instruments detection chains sensitive parts (e.g. detectors, preamplifiers input stages) can be well described through the overshielding transfer impedance concept.

To assess the coupling, one should consider separately :

- an external domain : the overshielding external surface with the ESD current flowing on
- an internal domain : the conductors internal to the overshielding considered as a multiconductor line referenced to the overshielding, considered as the ground plane

The current flowing in the external domain multiplied by the transfer impedance is then converted into distributed voltage sources in series on all the internal conductors (that is to say common mode voltage sources).

The result at the interface will be a voltage transient either between the ground lead and another lead of a sensitive part, or, because of the unbalance of impedances at the interface (cf. § 5.3) and the resulting poor CMRR, between any two leads of a sensitive part.

The corresponding peak power/duration should then be compared to the interface parts damage threshold in order to confirm the survival to a typical ESD and to assess the margin.

The logic of the external cryo-harness ESD assessment would then be the following :

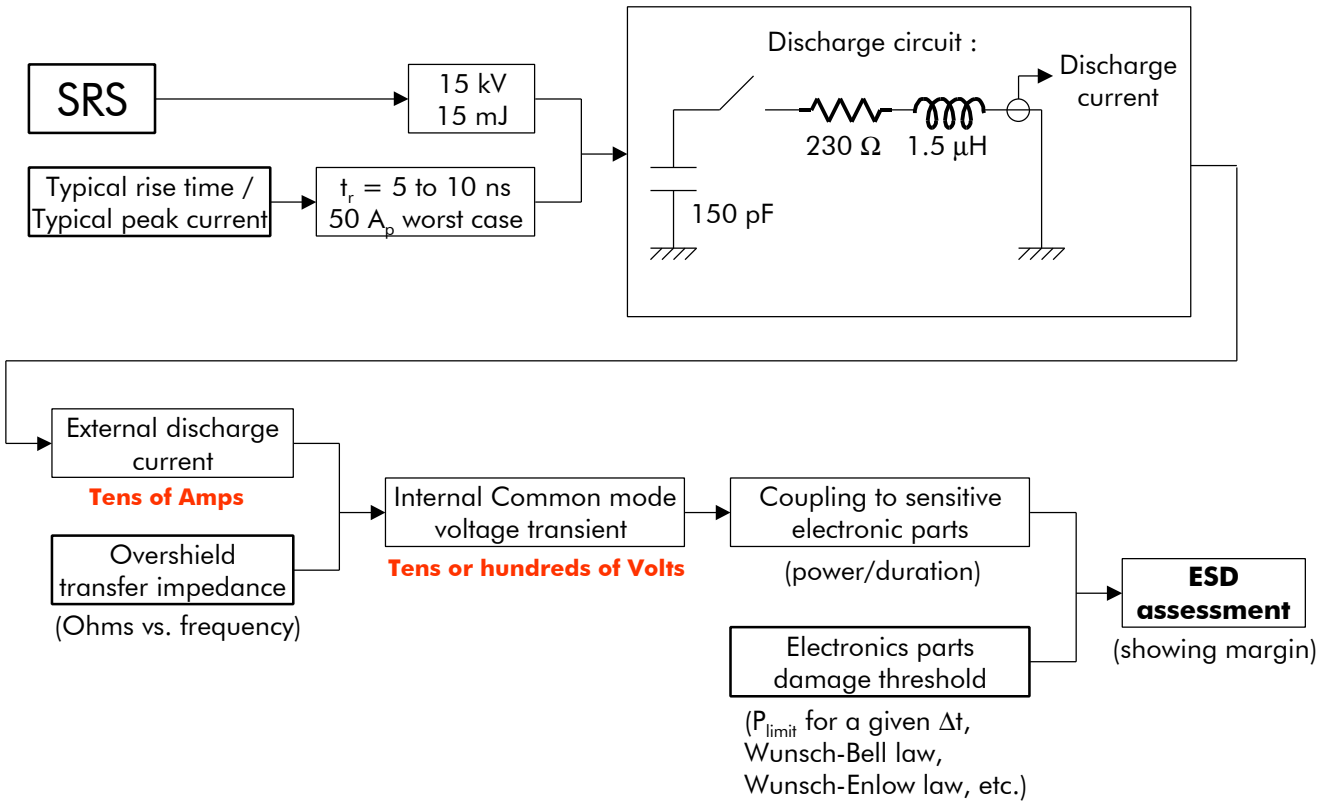

The last step of the assessment (damage threshold) is dealt with in § 5.9.3.

The discharge circuit characteristics and the Internal Common mode voltage transient order of magnitude shown in the previous block diagram were deduced from circuit simulation :

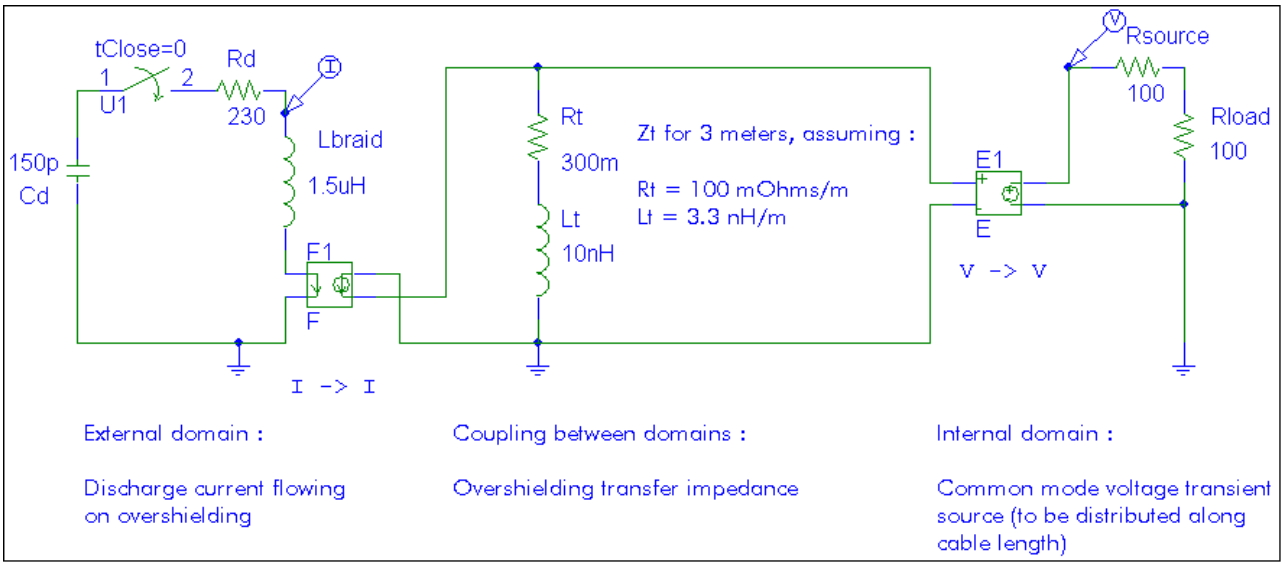

Note that the Z_t value taken into account is arbitrary (although not unrealistic a priori).

The resulting ESD current and corresponding internal common mode voltage transient are shown in the next figure :

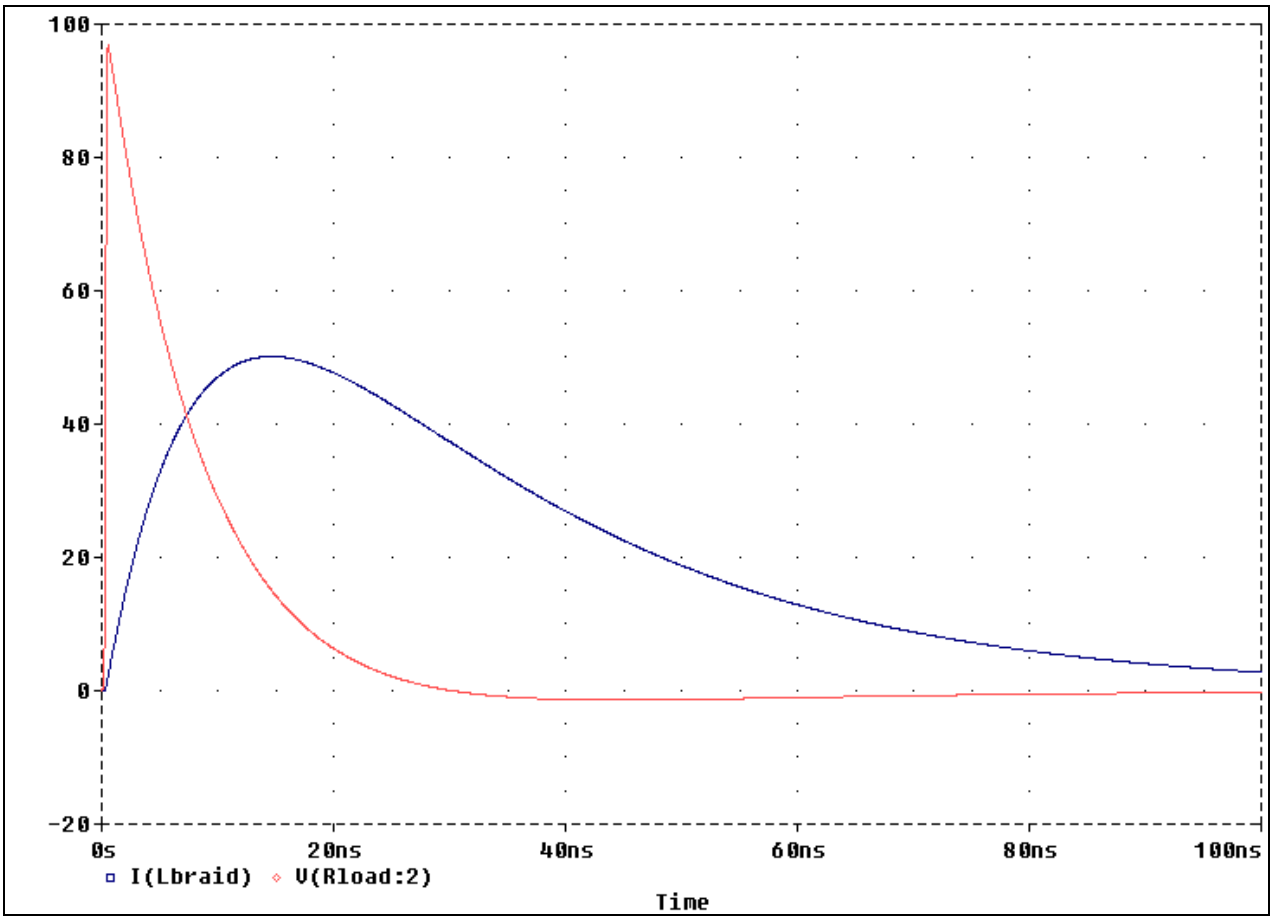

5.9.3 Circuits survival to ESD induced transients

Unlike the human ESD, specified in the Human Body Model (HBM) of the MIL-STD-883 (100 pF in series with 1500 Ω, to be connected directly to the tested interface), the current corresponding to a flight ESD is only limited by the impedance of the equivalent Thévenin generator as seen from the interface of interest, that is typically 50 to 200 Ω i.e. typically the characteristic impedance Z_C of the line.

So in order to assess the impact of a flight ESD induced voltage transient to an interface, one must not rely on the data based on the HBM (corresponding rather to a punch-through type of destruction, or dielectric failure), but must rather consider the energy dissipated into the interface semi-conductor circuit.
The theory allowing to handle this (thermal failure) was developed Wunsch and Bell.

The theory predicts that the asymptotic behaviour of the relationship between the failure power (P) and the time-to-failure (t) shows three different phases :

- adiabatic : P proportional to t^{-1} for transients shorter than ~100 ns
- semi-adiabatic : P proportional to $t^{-0.5}$ for transients between ~0.1 μs and 20 to 100 μs
- thermal balance : P independent from time for longer transient durations

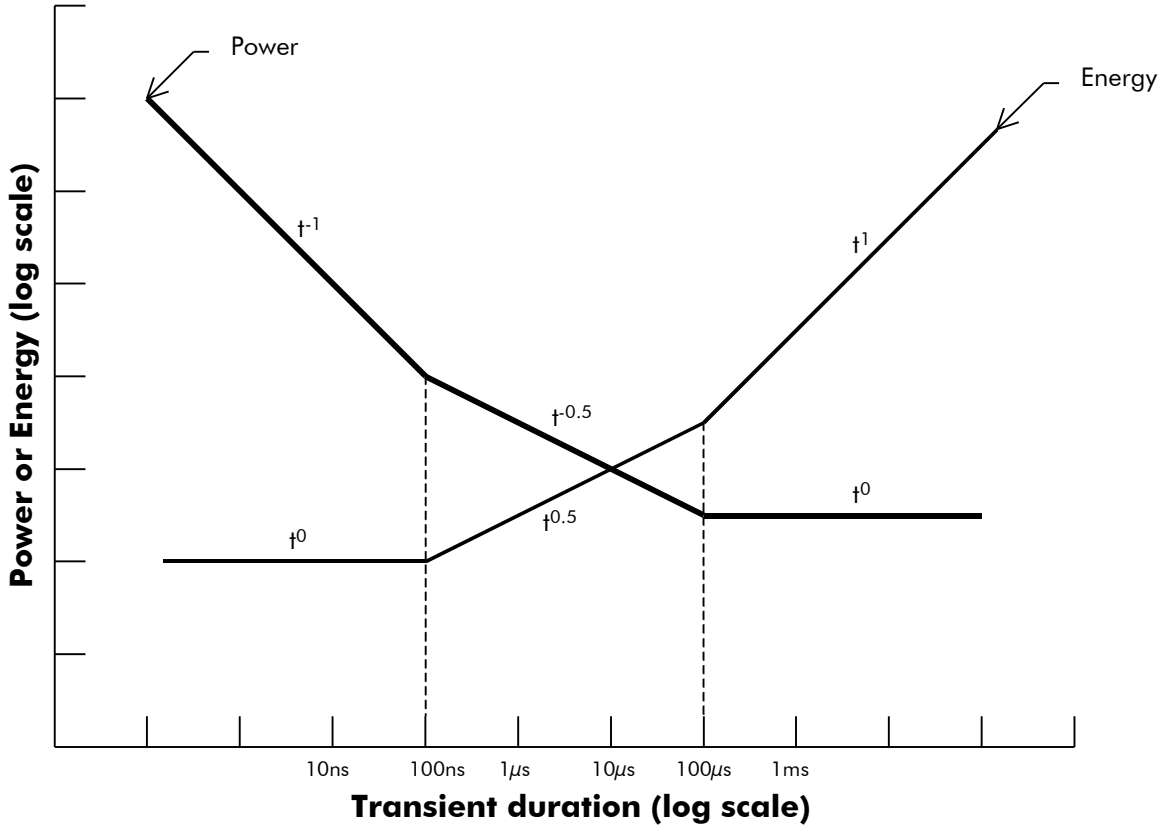

As far as ESD is concerned, the phase of interest is the semi-adiabatic one, involving the Wunsch constant K depending on the device of interest :

$P = Kt^{-0.5}$

For **discrete components**, Wunsch and Enlow have proposed to relate K to the component "rated power" (DC or CW maximum power admissible by the electronic part) as follows :

$$K = \begin{cases} 10 \times RP \text{ for } & RP \le 10W \\ 100 \quad \text{for } & 10 \le RP \le 100W \\ RP \quad \text{for } & RP \ge 100W \end{cases}$$

For the **integrated circuits**, Wunsch and Enlow have proposed a generic formula (independent of the technology) of failure power for times between 100 ns and 10 μs :

$P = At^{-B}$ with A = 87.6, B = 0.6, t in μs
This model represents the nominal expected failure level (50% confidence).
Other values of A were proposed for the lower confidence bounds :

Confidence	Value of A
90 %	18
95 %	11.5
99 %	4.95

For A = 4.95 (99 % confidence) and t = 100 ns, the failure energy level would be as low as **2 μJ**.

The Wunsch and Enlow model is meant to "give a conservative estimate of failure levels but not so overly conservative as to inordinately drive systems to overhardening".

Note 1 :
We consider wise to extend the semi-adiabatic zone up to a few tens of nanoseconds on the short times side for Integrated Circuits.

Note 2 :
All the previous transient durations and energy/power levels consider a square-shaped transient.
Cable response will rather be, classically, a damped sinus.
That is why even if the first peak of the ESD-induced common mode transient might be as short as 10 or 20 ns (cf. § 5.9.2), a 100 ns duration was considered to account for the harness resonance resulting in a damped sinus response (maybe conservative, as due to the high resistance of the cryo-harness, the resonance should be quickly damped).

Note 3 :
RF components, such as the ones in HIFI FPU (IF mixers and amplifiers) and in HIFI LOU, are not covered by the Wunsch and Enlow model and may have lower damage thresholds. This is to be assessed by HIFI (same comment for LFI on Planck).
JPL "LO ESD/EMC Test Plan", JPL/HIFI/PL/2001-001 mentions that "the LOU contains very sensitive planar GaAs Schottky diode base multipliers that are extremely susceptible to ESD".
From the same document § 5.2.2 the bias line inputs to the multiplier diodes in band 5 will be protected by two RC filters in series (100 Ω / 0.1 μF & 100 Ω / 200 pF).

5.9.4 Instruments external cryo-harness overshieldings assessment

In the frame of the EMC WG meetings, Herschel Instruments have been asked to specify their needs in terms of external cryo-harness overshieldings transfer impedance (H-P-ASPI-MN-810/1, due date 15/02/2002).

SPIRE :
No answer received (05/03/2002).

PACS :
Maximum Zt of 0.2 Ohms over the complete length over the frequency range from DC to 10 MHz.

HIFI :
No answer received (05/03/2002).

The order of magnitude of the energy transmitted to an interface circuit as a consequence of an ESD current flowing on the corresponding external cryo-harness overshielding can be calculated as follows :

$$Z_T \cdot I_{Overshield} = Z_{component} \cdot I_{Internal}$$

It must be noted that the DC impedance of the interface is to be considered carefully, the impedance relative to the transient phenomenon of interest may be significantly different, and in particular much lower.
The worst case for interface impedance occurs when it is equal to the ESD induced transient equivalent Thévenin source impedance (maximum energy transfer).
As mentioned in § 5.9.3, the typical value to take into account is 50 to 200 Ohms, that is to say the order of magnitude of the internal line characteristic impedance.
(Note : if the interface of interest is protected by a series resistance, it should then of course be taken into account).

With the a.m. approach, the worst case energy transferred to the interface component is :

$$W = \frac{\left(Z_T \cdot I_{Overshield}\right)^2}{4Z_C} \cdot \Delta t$$

Then assuming :

$Z_T.I_{overshield} = 100$ V
$Z_c = 100\ \Omega$
$\Delta t = 100$ ns

the energy value reached is **2.5 µJ**, that is about the same value as the one from the Wunsch and Enlow model for ICs calculated in the previous paragraph.

In the end we have shown that demonstrating the interface circuits survival to an ESD current flowing on the cryo-harness is not straightforward as :

- **a coarse analysis is not enough to demonstrate a big margin covering all possible cases (i.e. not enough to eliminate the problem a priori)**.
- the energy damage threshold of the devices of interest is not known, giving us no other choice than to rely on the Wunsch and Enlow models : if relevant, the damage threshold is **to be assessed by the Instruments**, especially whenever RF components are to be taken into account (e. g. in JPL "Technical note on multiplier protection circuits", JPL/HIFI/_TN/2001-001, RC filters are proposed to

protect bias lines inputs of the very fast and very small, and therefore very sensitive to ESD, submicron planar Schottky diodes used in the LO frequency multipliers. However the analysis relies on the human body model with 2 kV, that does not cover the characteristics of a flight ESD)

- the real overshielding Z_T is not known ; that is **to be assessed by Astrium for Herschel**

Concerning the Planck Instruments, HFI cryo-harness from the FPU to the JFET box and from the JFET box to the PAU is protected by a SST "bellow" that is understood to provide full optical coverage and continuity over 360° at the ends.

The same method as before can be used to assess the interface circuits survival to a structure ESD current. The main unknown is the bellows transfer impedance, to be assessed by HFI.

LFI cryo-harness transmitting FEM bias and phase switch bias to the FPU, and ensuring temperature acquisition is the probably the least shielded external cable, being a flat multiconductor cable protected only by two thin layers of metal on top and bottom, fortunately connected to chassis on both sides (FPU side and DAE lateral trays side.
Again the transfer impedance needs to be known to allow to propose an ESD assessment.
This is to be performed at a latter stage.

6. CONCLUSION

In the present analysis document, we have shown that intrinsic CS/CE margins exist between CS and CE specification on the primary power lines. The compliance of the various users of the 28 V primary power bus will guarantee the proper functioning of both spacecrafts once integrated.

In case of non compliance of an equipment or Instrument unit, the knowledge of the system margins will allow to manage the relaxations.

Concerning the RF compatibility issues, the compatibility of the spacecraft with the launcher should be ensured easily. More potentially critical are :

- HIFI compatibility with Herschel spacecraft telecommand reception : the radiated emission of the Instrument in the spacecraft TC receive band is still to be assessed (spec : 0 dBμV/m)
- SVM compatibility (more especially the TTC Rx) with HIFI in the Instrument IF band [4 – 8 GHz] : the system margins have been assessed according to various emission / susceptibility scenarii ; we are rather optimistic as HIFI is clearly willing to improve their FPU shielding efficiency, and on the other hand there are probably unknown hidden system margins related to the SVM – OB RF decoupling (actually difficult to assess)

The most serious EMC topic is the Instruments detection chains EMC assessment, involving both detectors output signals chains and bias lines.

The “rules” of detection chains protection against both low frequency and high frequency EMI have been recalled and explained.
It must be noted that the dimensioning coupling mode of EMI to the detection chains is the so-called “ground loop coupling” (GLC) which results in induced EMI common mode sources that in turn are converted into differential mode because of the imperfections of circuits balance and the frequency limitation of 0V isolation strategies. The EMC simulations that are being performed by the Instruments (with PSPICE or other software) should all aim at assessing the rejection of the EMI-induced CM noise (in other words the GLC).

Then the Instruments detection chains grounding strategies / concepts have been confronted with the a.m. “rules” and a preliminary assessment has been proposed. Means of protecting the sensitive signals against BF and HF EMI exist in the grounding of each Instrument and/or in the general design of each satellite (such as overshields, sapphire, etc.).

It should be noted that the maturity of EMC analyses of the detection chains by the various Instrument teams is very variable between different Instruments. Some of the Instruments have a clear grounding baseline and have already performed analyses and engineering tests. Some of them have not yet described clearly their grounding baseline (although they are working on it).

The Spacecraft survival to a typical ESD (required in the SRS) is also a very serious EMC matter as far as the detection chains are concerned, because in most cases a significant part of the cryo-harness is external.
On Herschel, the baseline Instruments design, that is also the baseline ASPI design is to protect the external cryo-harness by an overshielding.

Again the coupling mechanisms of a typical ESD to the sensitive Instruments electronics parts has been described. A simple but technically correct method has been proposed, that the Instruments can use to derive an assessment of their survival margin to an ESD.
Indeed, a quantitative analysis has shown that the margin demonstration necessitates more specific inputs than the ones available to ASPI today.
However on Herschel we are confident that, unless :

- the overshielding transfer impedance is significantly worse than assumed
- or some instrument parts having a damage threshold significantly worse than the Wunsch and Enlow model are not suitably protected

a safe ESD design should be reached (as long as the external cryo-harness is overshielded, needless to say).

END OF DOCUMENT

ANNEX 1

28V Bus Conducted Susceptibility Common mode Transient Specification Assessment

ALCATEL SPACE

28V Bus Conducted Susceptibility Common Mode Transient Specification Assessment

Rédigé par/Written by	Responsabilité-Service-Société Responsibility-Office-Company	Date	Signature
L. TROUGNOU	EMC – BO/EI/IP – Alcatel Space	05/06/01	
Vérifié par/Verified by			
Approbation/Approved			

Entité Emettrice : BO/EI/IP
(détentrice de l'original) :

ENREGISTREMENT DES EVOLUTIONS / CHANGE RECORDS

ISSUE	DATE	§ : DESCRIPTION DES EVOLUTIONS § : CHANGE RECORD	REDACTEUR AUTHOR
1	05/06/2001	First issue	L.T.

TABLE DES MATIÈRES / TABLE OF CONTENTS

LISTE DES FIGURES / LIST OF FIGURES

1. SCOPE

This note gives an evaluation of the common mode voltage transient liable to be created between return and chassis at a unit 28V power interface by a short circuit failure of another unit.

It was written in the frame of Herschel-Planck program in order to justify the common mode CS transient specification.

Two kinds of short circuits were considered :

- hot wire to return
- hot wire to chassis

A common mode CS transient specification should be derived from the from the analysis results in order to demonstrate by tests the system margin.

2. MODELS

The evaluation of the common mode voltage transient initiated by a short circuit of a user of the 28 V bus was done with simple PSPICE models.

The models are described on the following figures :

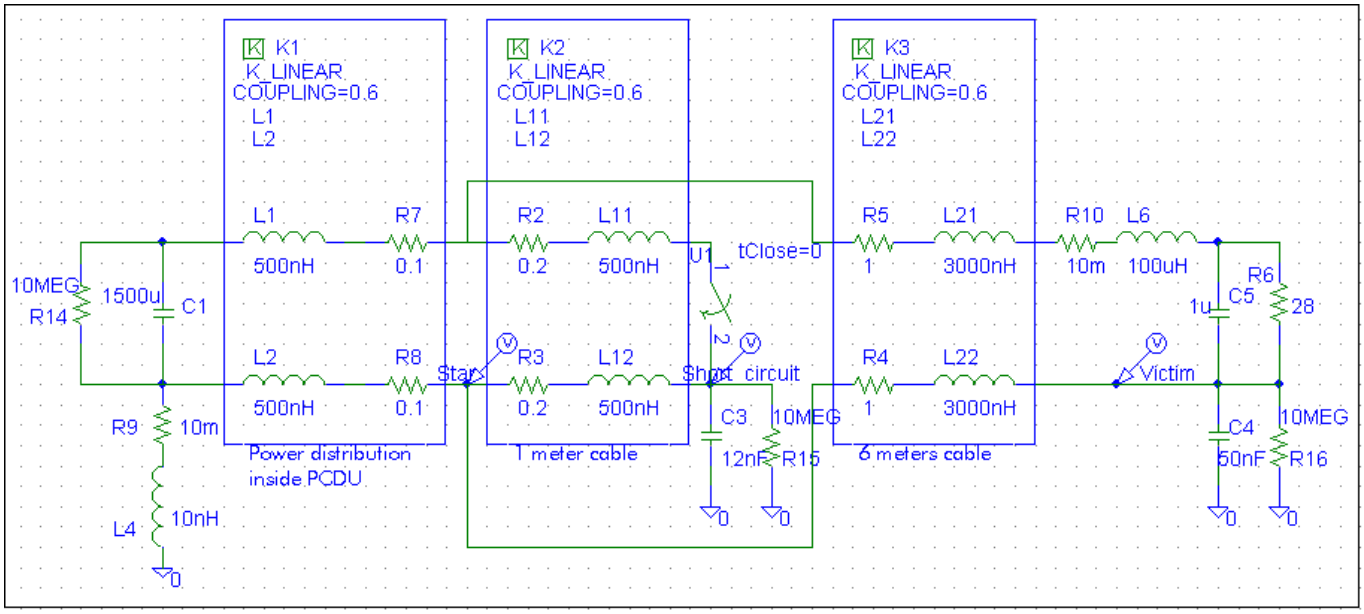

Figure 1 : model for hot wire to return short circuit

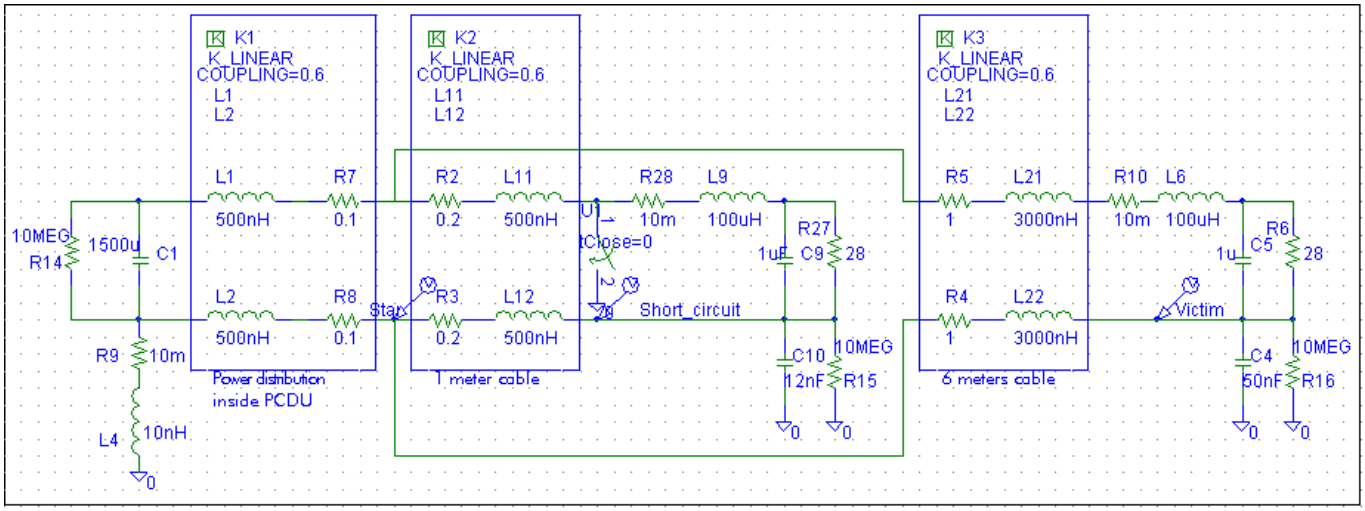

Figure 2 : model for hot wire to chassis short circuit

The elements are :

- the PCDU tank capacitor, pre-charged to 28V
- the distribution internal to the PCDU, modelled as 2 coupled inductance's
- the power line to the failing unit and to the victim unit
- some elements of the input filters of the failing unit and of the victim unit, especially the common mode capacitors

The LCL's are not modelled as we have no SPICE model of them yet but they are not expected to change radically the phenomenon at the first microseconds (i.e. voltage transients linked to quick current variation in the cable inductance's).

The PCDU internal link length and the failing unit cable length have been maximised and minimised respectively in order to be in a worst case, i.e. star point as far as possible from the tank capacitor and failing unit as close as possible to the star point. Cf. § 3 for the understanding of the phenomenon.

The resistance values of the cables may seem high but they have been chosen according to the voltage transient pseudo-frequency (cf. § 3).

The inductive aspect of the cables is modelled according to the following typical values :

- self inductance of each wire w.r.t chassis : L = 0.5 μH/m
- differential path self inductance : L_{diff} = 2(L-M) = 2L(1-K) = 0.4 μH/m supposing K = 0.6 with M : mutual inductance between wires and K = M/L coupling factor
- common mode path self inductance : L_{com} = (L+M)/2 = (L/2)*(1+K) = 0.4 μH/m

3. RESULTS

3.1 FAILURE EFFECT

The common mode transient voltage values at failing unit, star point, and victim unit respectively are presented on the two following figures :

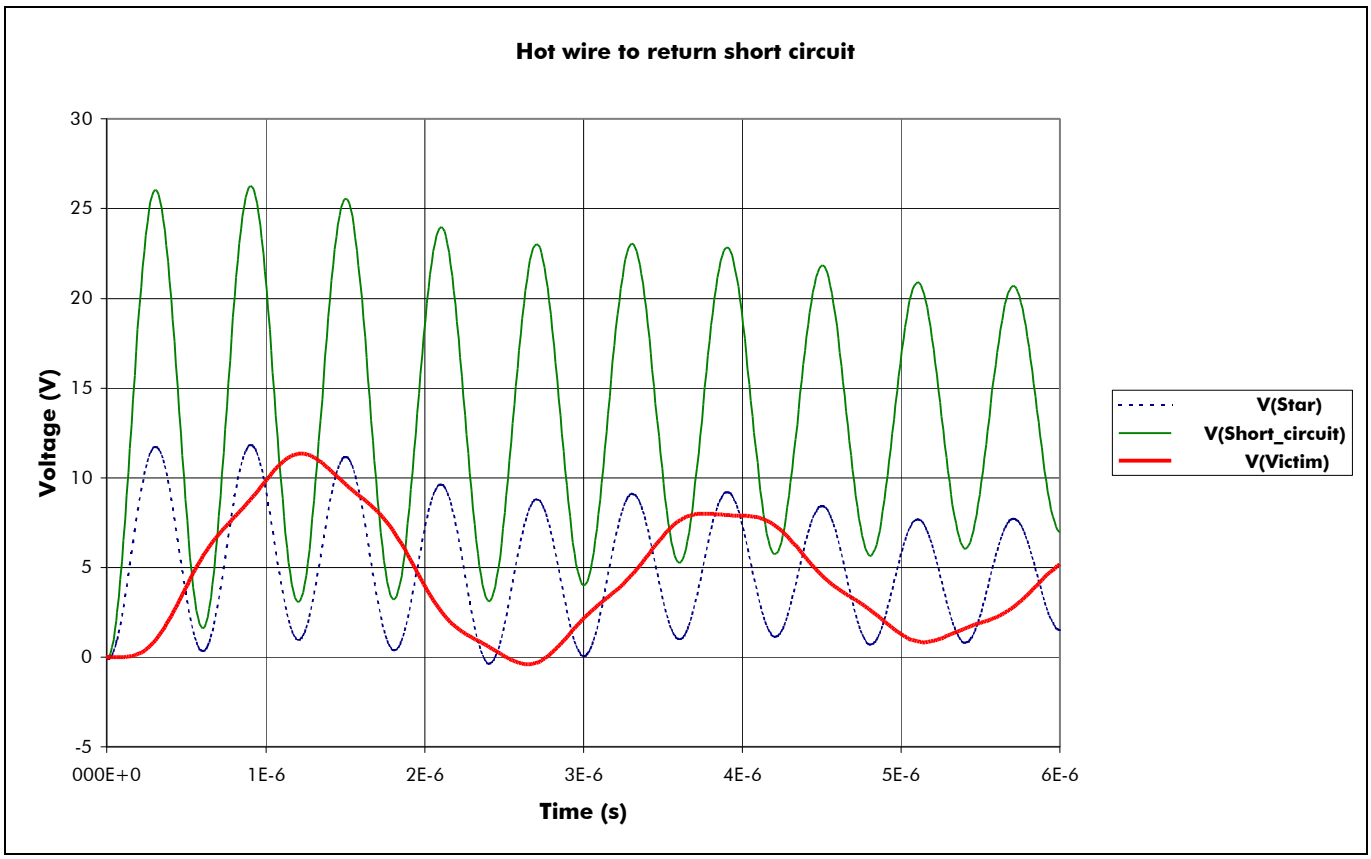

Figure 3 : results of hot wire to return short circuit

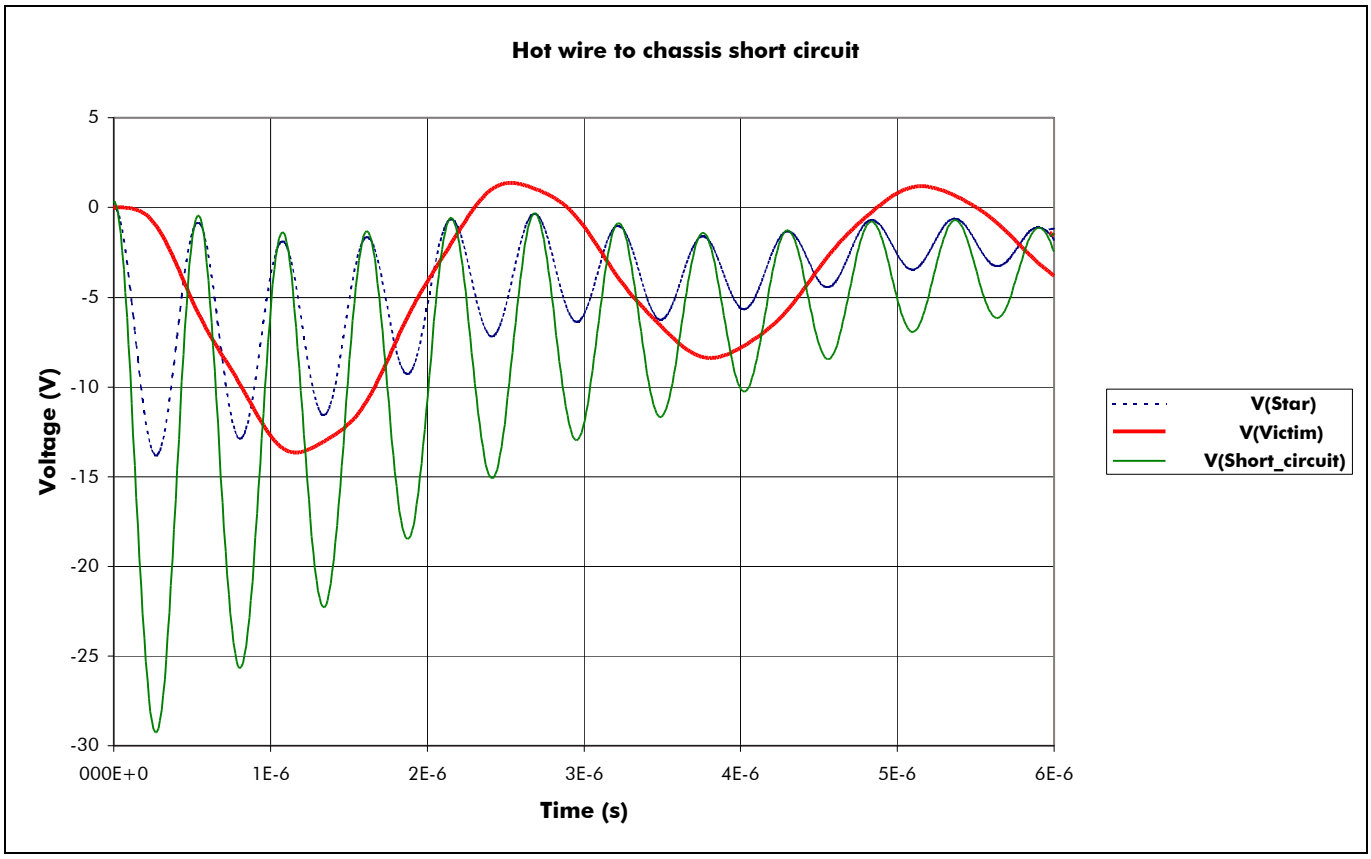

Figure 4 : results of hot wire to chassis short circuit

The phenomenon is roughly the following (case of short circuit to return) :

- Because of the equal inductance values between the cable linking the PCDU to the failure and the link internal to the PCDU linking the "star point" to the tank capacitor, the voltage transient value at star point is half the voltage transient value at failure point.
- The short circuit initiates common mode resonance phenomena between the common mode inductance's and the common mode capacitance's, that determine the transient pseudo-periods : in our example :
  - For the "victim" unit : 1/(2*pi*sqrt(50nF*2800nH)) ~ 425 kHz (about 2.35 μs duration).
  - For the failing unit : 1/(2*pi*sqrt(12nF*800nH)) ~ 1.6 MHz (about 0.6 μs duration)

  Note that the common mode capacitance's have been chosen with different values in order to feature this phenomenon by having clearly distinct resonance frequencies. 50 nF is the maximum allowed value according to the GDIR.

In the case of a short circuit to the chassis, the phenomenon is roughly the same but the transients are negative.

3.2 WORST CASE

Several cable lengths and common mode capacitance values have been tried and the worst case found was the following :

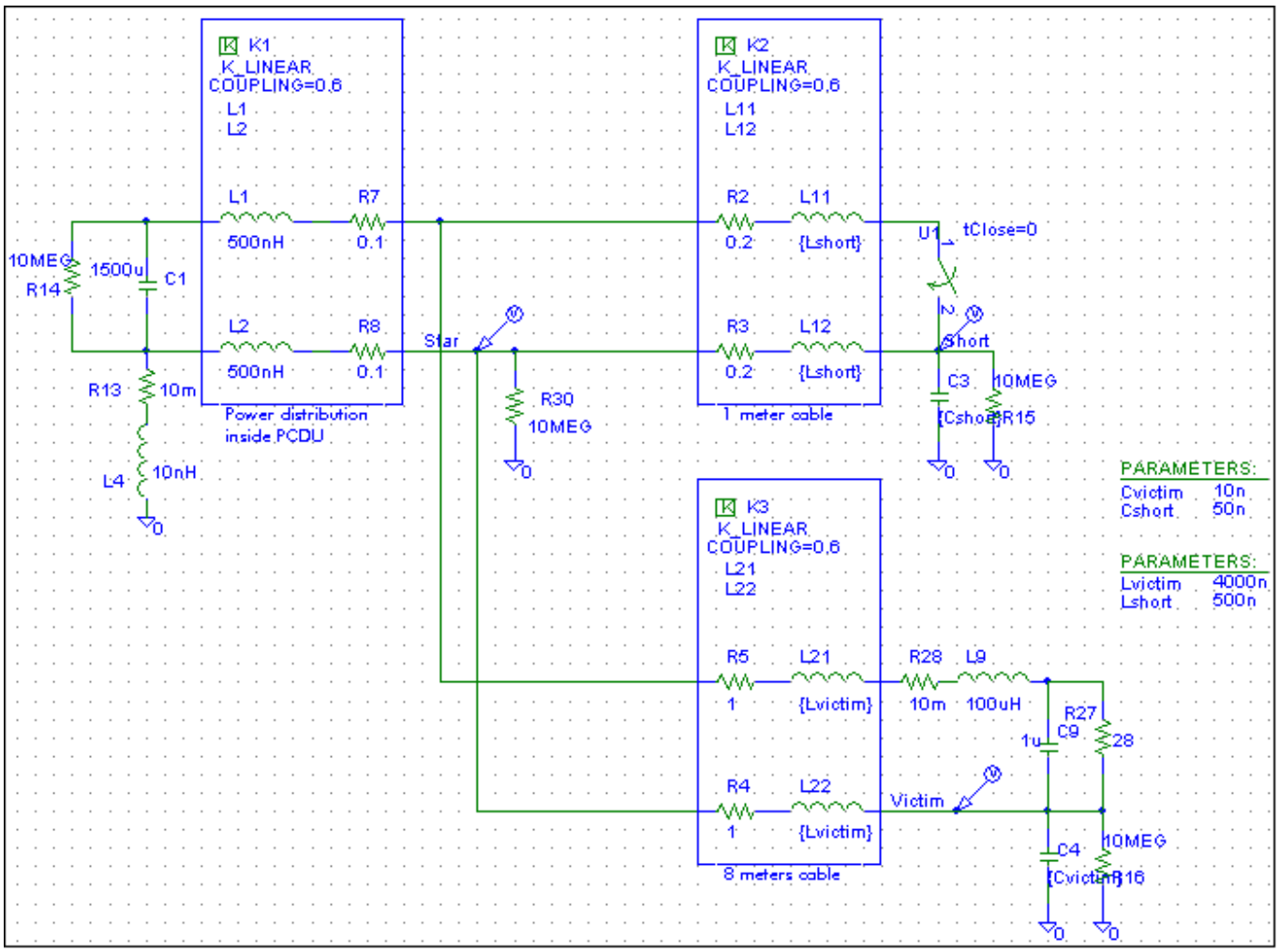

Figure 5 : worst common mode capacitance and cable length values

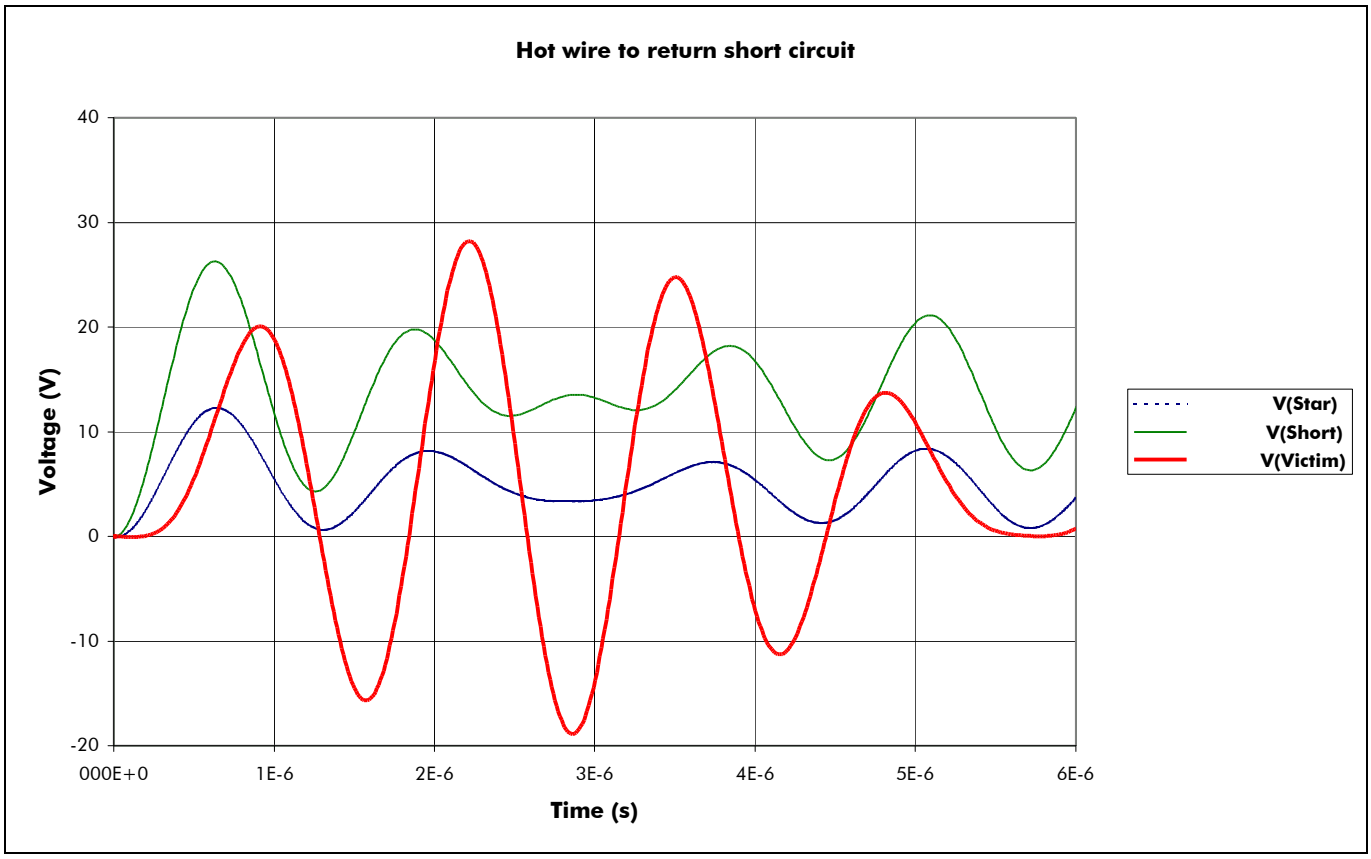

Figure 6 : results with worst common mode capacitance and cable length values

It must be noted that according to our hypotheses the voltage transient peak value at victim unit power input can be as high as 28 V_p.

4. CONCLUSIONS

1) Unless we demonstrate by a more accurate simulation that the transient characteristics from the presented simulations are pessimistic, we have to keep the CM CS transient amplitude already foreseen in the EMC specification, i.e. **28 V**.
   On the other hand, the 10 μs time specified so far seems too long, and should be reduced to ***5 µs*** (that would be sufficient to achieve a 6 dB margin), considering that the test equipment used to perform the "CS06" test from the MIL-STD (e.g. : SOLAR 8282) can generate 0.15 μs, 5μs and 10μs transients.

2) Common mode short circuit transients should be measured in the frame of PCDU qualification in order to demonstrate the system margin. The test set-up should include representative test cable length and common mode test capacitors. The following test set-up can be envisaged :

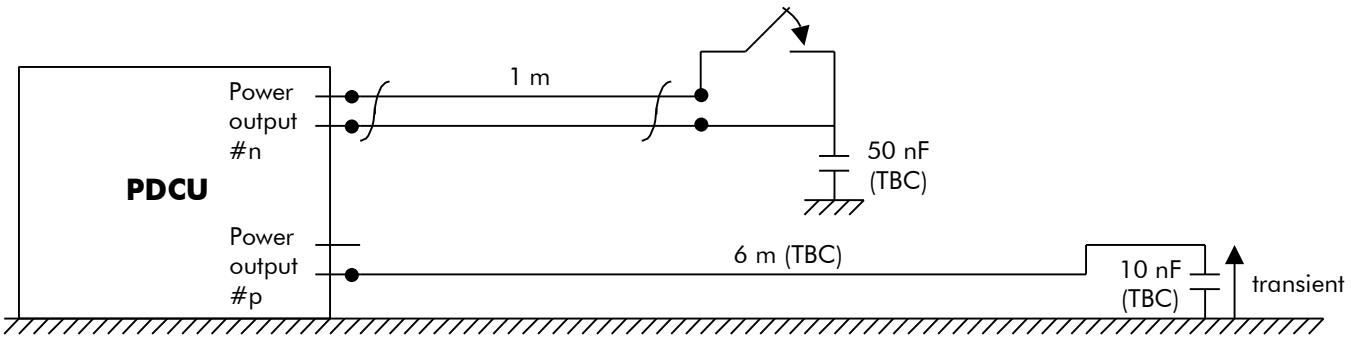

Figure 7 : PCDU CE common mode transient test set-up

FIN DE DOCUMENT
END OF DOCUMENT